

Quantum advantages for syndrome-aware noisy logical observable estimation

Kento Tsubouchi,^{1,*} Hyukgun Kwon,² Liang Jiang,³ and Nobuyuki Yoshioka^{4,†}

¹*Department of Applied Physics, University of Tokyo, 7-3-1 Hongo, Bunkyo-ku, Tokyo 113-8656, Japan*

²*Department of Physics and Astronomy, Sejong University, 209 Neungdong-ro Gwangjin-gu, Seoul 05006, Republic of Korea*

³*Pritzker School of Molecular Engineering, University of Chicago, Chicago, Illinois 60637, USA*

⁴*International Center for Elementary Particle Physics, University of Tokyo, 7-3-1 Hongo, Bunkyo-ku, Tokyo 113-0033, Japan*

Recent progress in fault-tolerant quantum computing suggests that leveraging error-syndrome information at the logical layer can substantially improve performance, including the estimation of logical observables from noisy states. In this work, based on quantum estimation theory, we develop an information-theoretic framework to quantify the utility of error syndromes for noisy logical observable estimation. We distinguish two operational regimes of such syndrome-aware protocols: *classical* protocols, in which the logical measurement basis is fixed and syndrome information is used only in classical post-processing, and *quantum* protocols, in which the logical quantum control can be tailored to depend on the observed error syndrome. For classical syndrome-aware protocols, we prove a universal limitation: on average, syndrome information can improve the effective logical error rate by at most a factor of two, implying at most a quadratic reduction in sampling overhead. In contrast, once syndrome-conditioned quantum control is permitted, we exhibit settings in which the effective logical error rate decays exponentially with the number of logical qubits. These findings provide fundamental guidance for designing future fault-tolerant architectures that actively exploit syndrome records rather than discarding them after decoding.

I. INTRODUCTION

Fault-tolerant quantum computing based on quantum error correction provides a powerful framework to suppress errors in quantum processors [1–4]. In quantum error correction, logical quantum information is encoded into a larger Hilbert space of physical qubits by introducing redundancy. Although physical qubits are subject to noise, one repeatedly measures redundant degrees of freedom to extract error syndromes, and then infers and corrects the underlying errors via decoding. With continuous experimental progress demonstrating quantum error correction [5–10], it is expected that sufficiently large-scale fault-tolerant devices will eventually enable reliable quantum computation with negligible logical errors.

However, especially in the early stages of fault-tolerant hardware development, limited resources make the implementation of full quantum error correction challenging. As a result, logical errors may remain in the logical state obtained after decoding, and it becomes necessary to design computational protocols that explicitly account for residual logical noise. In other words, one must estimate noiseless logical properties of interest from noisy logical states produced after decoding. For example, one can apply quantum error mitigation protocols [11–14] at the logical layer to further suppress logical errors [15–18].

Recently, there has been growing interest in protocols that go beyond using only the decoded logical state. By exploiting redundant information available at the physical layer—namely, the observed error syndromes—and constructing protocols conditioned on the syndrome record, one can further enhance the performance of the

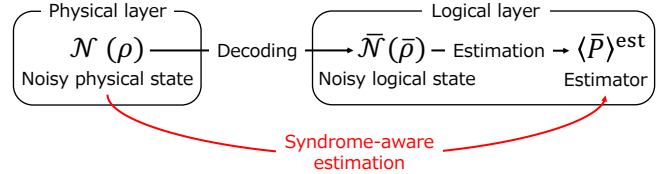


FIG. 1. Schematic illustration of syndrome-aware estimation. In conventional estimation protocols performed at the logical layer, one first obtains a noisy logical state by decoding a noisy physical state and then performs estimation using only the decoded logical state, while the error syndromes are not explicitly used at the estimation stage. In contrast, syndrome-aware estimation protocols explicitly incorporate the error syndromes into the estimation procedure, and can be viewed as a joint implementation of decoding and estimation.

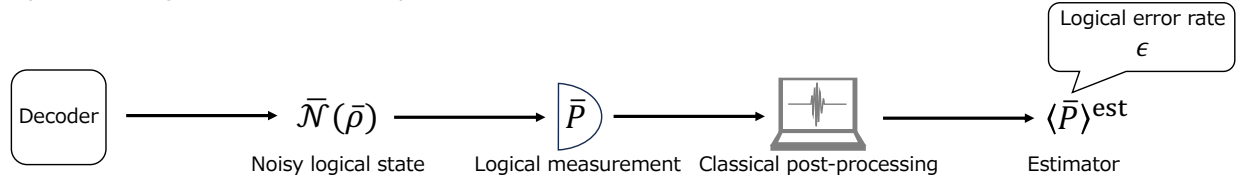
estimation (Fig. 1). For example, by estimating the logical error probability conditioned on the observed syndromes and post-selecting runs with low estimated error probability, one can further suppress the logical error rate and improve the estimation performance [19–25]. Moreover, syndrome-aware quantum error mitigation [9, 26–28], which performs post-processing conditioned on the observed syndromes, can reduce sampling overhead and improve estimation accuracy compared to error-mitigation protocols that do not use syndrome information.

In such a setting, a natural question is how far syndrome information can improve logical-layer estimation. While the syndrome record provides additional information about residual logical noise, it is not obvious what ultimate performance is achievable once we allow the estimation procedure to be conditioned on the observed syndrome. Existing information-theoretic limitations for

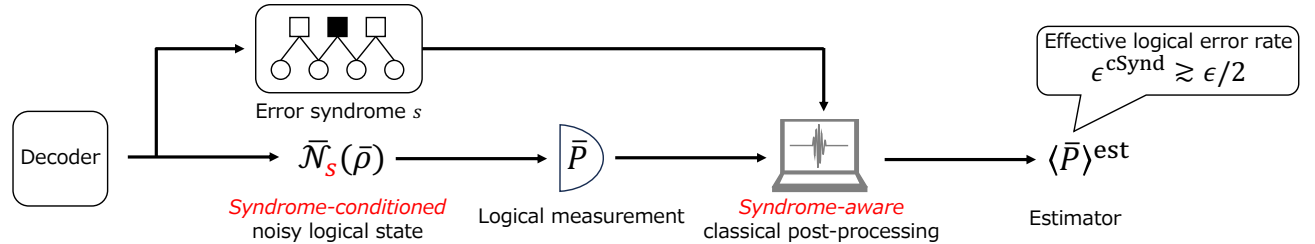
* tsubouchi@noneq.t.u-tokyo.ac.jp

† ny.nobuyoshioka@gmail.com

(a) Syndrome-agnostic estimation protocol



(b) Classical syndrome-aware estimation protocol



(c) Quantum syndrome-aware estimation protocol

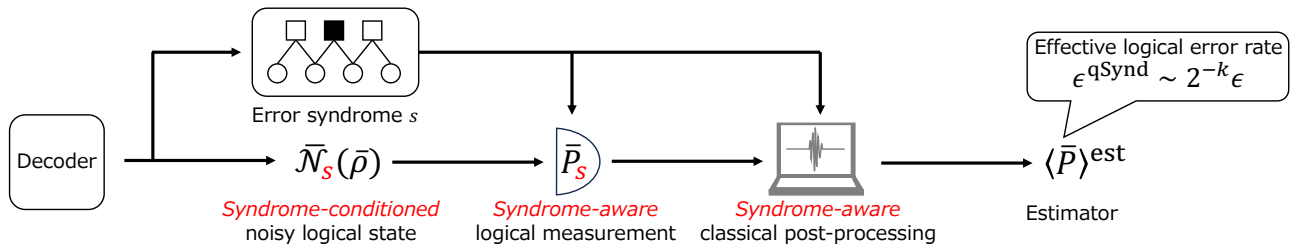


FIG. 2. Schematic illustration of syndrome-agnostic and syndrome-aware estimation protocols. (a) In the syndrome-agnostic estimation protocol, the decoder outputs an averaged noisy logical state, and we perform a fixed logical measurement on this state followed by classical post-processing to estimate a noiseless observable. The error-syndrome information is not used in either the measurement or the classical post-processing. The effect of the error on the resulting estimator is characterized by a logical error rate ϵ . (b) In the classical syndrome-aware estimation protocol, we assume that the decoder outputs the observed error syndrome s together with a syndrome-conditioned noisy logical state. The error-syndrome information is used only at the classical post-processing stage, while the logical measurement basis does not depend on the observed syndrome s . We characterize the effect of the error in this scenario by the *effective logical error rate* ϵ^{cSynd} , which is lower-bounded by one half of the original logical error rate ϵ on average. (c) In the quantum syndrome-aware estimation protocol, we again assume that the decoder outputs the observed error syndrome s and a syndrome-conditioned noisy logical state. Unlike the classical protocol, we additionally allow the logical measurement basis to depend on s , followed by syndrome-aware classical post-processing. This allows the effective logical error rate ϵ^{qSynd} to be exponentially smaller than the original logical error rate ϵ as a function of the number of logical qubits k .

estimation from noisy quantum states [29–32] do not directly answer this question, because they treat the estimator as acting only on a single noisy quantum state and do not incorporate the extra information carried by the syndrome record. Consequently, it remains unclear how to fully exploit syndrome information and what the fundamental limits are in this setting. Establishing fundamental limits in this syndrome-aware setting is therefore essential for assessing the true value of syndrome data and for designing fault-tolerant architectures and mitigation protocols that achieve reliable estimation with substantially reduced resources.

In this work, based on quantum estimation theory [33–35], we develop a theoretical framework for quantifying

how useful error-syndrome information is for estimating logical observables from noisy states. We first define *syndrome-agnostic* estimation protocols as those that perform estimation directly on the decoded noisy logical state without using the syndrome record (Fig. 2(a)). We then consider two operational regimes for *syndrome-aware* protocols: (i) *classical* syndrome-aware protocols, where the logical measurement basis is fixed for all syndromes and syndrome information is used only in classical post-processing (Fig. 2(b)); and (ii) *quantum* syndrome-aware protocols, where the logical measurement (and more generally, logical quantum control) can be tailored to depend on the observed syndrome (Fig. 2(c)). We analyze and compare the Fisher infor-

mation across these three settings. To quantify the gain from syndrome information, we introduce an *effective logical error rate*, defined as the logical error rate of a syndrome-agnostic protocol that would yield the same Fisher information as a given syndrome-aware protocol.

Our main message is that the impact of syndrome information depends qualitatively on whether syndrome-conditioned quantum control is available. We first establish a universal limitation for classical syndrome-aware protocols. While syndrome-aware classical post-processing can reduce the impact of errors compared to syndrome-agnostic protocols, we prove that the effective logical error rate can be improved, on average, by at most a factor of two compared to the logical error rate of an optimal decoder. This implies that the sampling overhead can be improved at most quadratically by using the syndrome record classically, and hence the exponential overhead inherent to quantum error mitigation [29–32] cannot be avoided. In contrast, once quantum syndrome-aware protocols are permitted—i.e., the measurement basis can be adapted to the observed syndromes—the above limitation by classical protocol can be violated. Concretely, for a broad class of even-distance stabilizer codes, we exhibit settings in which the effective logical error rate becomes exponentially smaller than the logical error rate as the number of logical qubits increases.

These results establish a clear separation between what can and cannot be achieved by leveraging error-syndrome information for noisy logical observable estimation. On the one hand, they provide a general no-go statement showing that syndrome-dependent classical post-processing alone offers only limited improvements. On the other hand, they identify syndrome-conditioned quantum control—in particular, adapting the measurement basis to the observed syndrome record—as the key ingredient that enables genuine asymptotic advantages, including exponential improvements with the number of logical qubits. More broadly, our framework offers a unified, information-theoretic way to quantify the utility of error-syndrome information, and provides fundamental guidance for designing future fault-tolerant protocols that actively exploit error syndromes rather than discarding them after decoding.

The remainder of the paper is organized as follows. In Sec. II, we review basic tools from classical and quantum estimation theory that underpin our framework. In Sec. III, we introduce the problem setup and define syndrome-agnostic as well as classical and quantum syndrome-aware estimation protocols. In Sec. IV, we analyze syndrome-agnostic protocols by deriving the corresponding Fisher information, which serves as a baseline for comparison. In Sec. V, we establish fundamental limitations of classical syndrome-aware protocols by deriving a lower bound on the effective logical error rate. In Sec. VI, we demonstrate exponential advantages of quantum syndrome-aware protocols. Finally, we summarize our contributions and discuss future directions in Sec. VII.

II. PRELIMINARIES

In this section, we summarize basic tools from classical and quantum estimation theory [33–35] that underpin our framework. In Sec. II A, we review classical estimation theory for a classical probability distribution parameterized by a single unknown parameter. In Sec. II B, we review quantum estimation theory for a quantum state parameterized by multiple unknown parameters.

A. Single-parameter classical estimation theory

Consider a classical probability distribution $\Pr(x|\theta)$ parameterized by an unknown parameter θ . Given N samples x_1, \dots, x_N drawn independently from $\Pr(x|\theta)$, we aim to construct an unbiased estimator θ^{est} of θ . Here, an estimator is unbiased if its expectation value equals the true parameter value, i.e., $\mathbb{E}[\theta^{\text{est}}] = \theta$. In this setting, the precision of the unbiased estimation is characterized by the *classical Fisher information*

$$F_\theta = \sum_x \frac{1}{\Pr(x|\theta)} (\partial_\theta \Pr(x|\theta))^2. \quad (1)$$

Indeed, the classical Fisher information provides the achievable lower bound on the variance $\text{Var}[\theta^{\text{est}}]$ of the unbiased estimator θ^{est} through the *Cramér–Rao bound*

$$\text{Var}[\theta^{\text{est}}] \geq \frac{1}{N} F_\theta^{-1}. \quad (2)$$

In the asymptotic regime $N \rightarrow \infty$, the asymptotically unbiased estimator that attains the Cramér–Rao bound is given by the maximum-likelihood estimator,

$$\theta^{\text{est}} = \arg \max_{\theta} \prod_{i=1}^N \Pr(x_i|\theta) = \arg \max_{\theta} \sum_{i=1}^N \log \Pr(x_i|\theta). \quad (3)$$

Next, consider a joint distribution of the form $\Pr(x, s|\theta) = p_s \Pr(x|s, \theta)$, where one first observes s with probability p_s and then observes x drawn from the conditional distribution $\Pr(x|s, \theta)$. If p_s is independent of θ , the classical Fisher information of $\Pr(x, s|\theta)$ decomposes as

$$F_\theta = \sum_s p_s F_\theta^{(s)}, \quad (4)$$

where $F_\theta^{(s)}$ denotes the Fisher information of the conditional distribution $\Pr(x|s, \theta)$. In our setting, s corresponds to the error syndrome, and $\Pr(x|s, \theta)$ is the outcome distribution of a logical measurement performed on the syndrome-conditioned noisy logical state.

B. Multi-parameter quantum estimation theory

Consider a quantum state $\bar{\rho}(\theta)$ parameterized by m unknown parameters $\theta = (\theta_1, \dots, \theta_m)$. Since we mainly

deal with logical operators, we denote operators acting on the logical Hilbert space by $\bar{\cdot}$, while ordinary (non-operator) quantities such as probability distributions and Fisher information matrices are written without $\bar{\cdot}$. Given N copies of $\bar{\rho}(\boldsymbol{\theta})$, we aim to construct an unbiased estimator θ_i^{est} of θ_i . We define the *symmetric logarithmic derivative* (SLD) operator \bar{L}_i by

$$\partial_{\theta_i} \bar{\rho}(\boldsymbol{\theta}) = \frac{1}{2} \{ \bar{\rho}(\boldsymbol{\theta}), \bar{L}_i \}, \quad (5)$$

and the (SLD) quantum Fisher information matrix $J \in \mathbb{R}^{m \times m}$ by

$$J_{ij} = \text{tr} \left[\bar{\rho}(\boldsymbol{\theta}) \frac{1}{2} \{ \bar{L}_i, \bar{L}_j \} \right]. \quad (6)$$

For a single parameter θ_i in the multi-parameter setting, we define the corresponding *quantum Fisher information* as

$$J_{\theta_i} = \frac{1}{(J^{-1})_{ii}}. \quad (7)$$

Then, the achievable lower bound on the variance $\text{Var}[\theta_i^{\text{est}}]$ of the unbiased estimator θ_i^{est} is given by the *quantum Cramér–Rao bound*

$$\text{Var}[\theta_i^{\text{est}}] \geq \frac{1}{N} J_{\theta_i}^{-1}. \quad (8)$$

In the asymptotic regime $N \rightarrow \infty$, an asymptotically unbiased estimator that attains the quantum Cramér–Rao bound can be constructed by first performing a measurement in the eigenbasis of the operator

$$\sum_j (J^{-1})_{ij} \bar{L}_j, \quad (9)$$

and then applying a maximum-likelihood estimator to the resulting classical data [36]. If the operator $\sum_j (J^{-1})_{ij} \bar{L}_j$ depends on the unknown parameters $\boldsymbol{\theta}$, one may use an adaptive two-step strategy: measure \sqrt{N} copies to obtain a rough estimate of $\boldsymbol{\theta}$, and then measure the remaining $N - \sqrt{N}$ copies in the eigenbasis of $\sum_j (J^{-1})_{ij} \bar{L}_j$ evaluated at the rough estimate [37, 38].

The discussion above assumes that all parameters $\boldsymbol{\theta} = (\theta_1, \dots, \theta_m)$ are unknown, so that the parameters other than θ_i act as nuisance parameters [36]. If, instead, all parameters except θ_i are known, the achievable lower bound is given by

$$\text{Var}[\theta_i^{\text{est}}] \geq \frac{1}{N} (J_{ii})^{-1}, \quad (10)$$

and the optimal measurement is the one that diagonalizes the SLD operator \bar{L}_i . An important point is that the optimal measurement generally depends on whether the other parameters are treated as known or unknown.

Finally, consider a classical–quantum state of the form

$$\sum_s p_s |s\rangle\langle s| \otimes \bar{\rho}^{(s)}(\boldsymbol{\theta}), \quad (11)$$

where p_s is independent of $\boldsymbol{\theta}$. Let $\bar{L}_i^{(s)}$ and $J^{(s)}$ denote the SLD operators and quantum Fisher information matrices associated with $\bar{\rho}^{(s)}(\boldsymbol{\theta})$. Then, the SLD operators and quantum Fisher information matrix for the classical–quantum state can be written as

$$\bar{L}_i = \sum_s |s\rangle\langle s| \otimes \bar{L}_i^{(s)}, \quad J = \sum_s p_s J^{(s)}, \quad (12)$$

and hence

$$J_{\theta_i} = \frac{1}{((\sum_s p_s J^{(s)})^{-1})_{ii}}. \quad (13)$$

Accordingly, an asymptotically optimal measurement for estimating θ_i is given by measuring s first and then, conditioned on s , measuring $\bar{\rho}^{(s)}(\boldsymbol{\theta})$ in the eigenbasis of $\sum_j (J^{-1})_{ij} \bar{L}_j^{(s)}$. Note that if one had access only to copies of a fixed conditional state $\bar{\rho}^{(s)}(\boldsymbol{\theta})$, the corresponding optimal measurement would instead involve $\sum_j ((J^{(s)})^{-1})_{ij} \bar{L}_j^{(s)}$. Thus, the optimal measurement for a given branch s generally depends on the presence of the other branches $\bar{\rho}^{(s')}(\boldsymbol{\theta})$ and their weights. In the main text, we interpret s as the error syndrome, and $\bar{\rho}^{(s)}(\boldsymbol{\theta})$ as the noisy logical state conditioned on the syndrome s .

III. PROBLEM SETUP

In this section, we describe the problem setup considered throughout this paper. Consider the task of preparing a k -qubit logical state

$$\bar{\rho}(\boldsymbol{\theta}) = \frac{1}{2^k} \left(\bar{I} + \sum_{i=1}^{4^k-1} \theta_i \bar{P}_i \right), \quad (14)$$

parameterized by an (unnormalized) generalized Bloch vector $\boldsymbol{\theta} = (\theta_1, \dots, \theta_{4^k-1})$ [39], and estimating the expectation value of a logical Pauli operator \bar{P}_i . Here, operators with $\bar{\cdot}$ represent operators of a k -qubit logical system: $\{\bar{P}_i\}_{i=0}^{4^k-1}$ denotes the set of k -qubit Pauli operators, with $\bar{P}_0 = \bar{I}$ the k -qubit identity operator. Since $\text{tr}[\bar{\rho}(\boldsymbol{\theta}) \bar{P}_i] = \theta_i$, this task is equivalent to estimating the parameter θ_i . For simplicity, we restrict to unbiased estimation of θ_i , and denote the unbiased estimator of θ_i as θ_i^{est} .

When a quantum device is affected by noise, we encode this logical state into an n -qubit physical state using an $[[n, k, d]]$ stabilizer code. After the physical noise affects the physical state, we perform syndrome measurements and then decode the noisy physical state, resulting in a noisy logical state

$$\bar{\mathcal{N}}(\bar{\rho}(\boldsymbol{\theta})) = \frac{1}{2^k} \left(\bar{I} + \sum_{i=1}^{4^k-1} (1 - 2\epsilon_i) \theta_i \bar{P}_i \right). \quad (15)$$

Here, we assume that the residual logical noise is Pauli noise, and ϵ_i is the logical error rate defined as the probability that a logical Pauli error anti-commuting with \bar{P}_i

occurs. To estimate θ_i , we perform a logical measurement of \bar{P}_i on $\mathcal{N}(\bar{\rho}(\boldsymbol{\theta}))$ and classically post-process the measurement outcomes to mitigate the effect of logical errors.

In such an estimation protocol, one performs identical operations on the decoded noisy logical state regardless of the observed error syndrome. In other words, the protocol does not use syndrome information, and we call it a *syndrome-agnostic estimation protocol* (Fig. 2(a)). Meanwhile, recent works have pointed out that using error-syndrome information at the logical-layer estimation stage can further boost performance, for example by post-selecting runs with low estimated logical error probability [19–25] or by performing classical post-processing conditioned on the observed syndrome [9, 26–28]. We call such protocols *syndrome-aware estimation protocols*. By incorporating syndrome information at the estimation stage, one can exploit information from the physical layer that would otherwise be discarded after decoding to improve the estimation of logical observables. Indeed, in Appendix A, we show that estimation performed directly on the noisy physical state is equivalent to a syndrome-aware estimation protocol, which justifies the schematic in Fig. 1.

To model syndrome-aware estimation protocols, we represent the decoder output as the observed error syndrome s together with a syndrome-conditional noisy logical state (Fig. 2(b),(c)). Concretely, we model the decoder output as a classical–quantum state

$$\sum_{s \in \mathcal{S}} p_s |s\rangle\langle s| \otimes \bar{\mathcal{N}}_s(\bar{\rho}(\boldsymbol{\theta})). \quad (16)$$

Here, s labels the syndrome, \mathcal{S} is the set of possible error syndromes, p_s is the probability of obtaining syndrome s , and $\bar{\mathcal{N}}_s$ is the logical noise channel conditioned on s , defined as

$$\bar{\mathcal{N}}_s(\bar{\rho}(\boldsymbol{\theta})) = \frac{1}{2^k} \left(\bar{I} + \sum_{i=1}^{4^k-1} (1 - 2\epsilon_{i,s}) \theta_i \bar{P}_i \right). \quad (17)$$

We assume that each syndrome-conditioned logical noise channel $\bar{\mathcal{N}}_s$ is also Pauli, and $\epsilon_{i,s}$ denotes the probability that a logical Pauli error anti-commuting with \bar{P}_i occurs when conditioned on the error syndrome s .

Under this definition, a syndrome-aware estimation protocol is an estimation procedure performed on the classical–quantum state $\sum_s p_s |s\rangle\langle s| \otimes \bar{\mathcal{N}}_s(\bar{\rho}(\boldsymbol{\theta}))$. In contrast, a syndrome-agnostic estimation protocol is an estimation procedure performed on the averaged noisy logical state $\bar{\mathcal{N}}(\bar{\rho}(\boldsymbol{\theta}))$, where the syndrome information is traced out:

$$\bar{\mathcal{N}} = \sum_{s \in \mathcal{S}} p_s \bar{\mathcal{N}}_s, \quad \epsilon_i = \sum_{s \in \mathcal{S}} p_s \epsilon_{i,s}. \quad (18)$$

Therefore, to quantify the information gain from utilizing error-syndrome information in estimation, it suffices

to compare the information contained in the classical–quantum state $\sum_s p_s |s\rangle\langle s| \otimes \bar{\mathcal{N}}_s(\bar{\rho}(\boldsymbol{\theta}))$ with that in the averaged state $\bar{\mathcal{N}}(\bar{\rho}(\boldsymbol{\theta}))$.

In the following, we consider two operational regimes for syndrome-aware protocols: (i) *classical* syndrome-aware protocols, where a fixed logical measurement of \bar{P}_i is applied to $\bar{\mathcal{N}}_s(\bar{\rho}(\boldsymbol{\theta}))$ for all s regardless of the observed syndrome and the syndrome information is used only in classical post-processing (Fig. 2(b)); and (ii) *quantum* syndrome-aware protocols, where the logical measurement basis is allowed to depend on the observed syndrome s (Fig. 2(c)). For the classical regime, we analyze the classical Fisher information of the outcome distribution obtained by measuring the classical–quantum state $\sum_s p_s |s\rangle\langle s| \otimes \bar{\mathcal{N}}_s(\bar{\rho}(\boldsymbol{\theta}))$. For the quantum regime, we analyze the quantum Fisher information of the same classical–quantum state. From these Fisher informations, we introduce an *effective logical error rate* to quantify the gain from syndrome information. The effective logical error rate is defined as the logical error rate of a syndrome-agnostic protocol that would yield the same classical/quantum Fisher information as a given classical/quantum syndrome-aware protocol. Our goal is to characterize how small the effective logical error rate can be, depending on which class of syndrome-aware protocol is allowed.

We conclude this section with several remarks on our assumptions. First, for the target operator \bar{P}_i , we assume $0 \leq \epsilon_{i,s} \leq 1/2$ for all $s \in \mathcal{S}$. This can be enforced by, for each syndrome s , choosing whether a logical Pauli error commuting with \bar{P}_i or anti-commuting with \bar{P}_i is more likely under s . This choice corresponds to using a degenerate quantum maximum-likelihood decoder [40–42] with respect to the logical observable \bar{P}_i , and then $\epsilon_i = \sum_s p_s \epsilon_{i,s}$ represents the logical error rate induced by this decoder. In the following, we refer to the degenerate quantum maximum-likelihood decoder simply as the maximum-likelihood decoder. Second, we assume a single-round code-capacity noise model, where the ideal physical state is affected by a single layer of physical noise, followed by a single round of noiseless syndrome measurement. Nevertheless, our framework extends to more general circuit-level noise models on Clifford circuits by interpreting $s \in \mathcal{S}$ as a full syndrome record and $\bar{\mathcal{N}}_s(\bar{\rho}(\boldsymbol{\theta}))$ as the logical state at the end of the circuit, as long as the circuit noise can be modeled as Pauli noise.

IV. FISHER INFORMATION ANALYSIS FOR SYNDROME-AGNOSTIC PROTOCOLS

In this section, we analyze the Fisher information for syndrome-agnostic estimation protocols, in which error-syndrome information is not used at the logical-layer estimation stage (Fig. 2(a)). As discussed in Sec. III, a syndrome-agnostic protocol performs estimation on the averaged noisy logical state $\bar{\mathcal{N}}(\bar{\rho}(\boldsymbol{\theta}))$. Equivalently, given N copies of $\bar{\mathcal{N}}(\bar{\rho}(\boldsymbol{\theta}))$, the goal is to construct an unbi-

ased estimator θ_i^{est} of the parameter θ_i . Therefore, the ultimate precision limit and sampling overhead of the syndrome-agnostic protocol can be analyzed using the quantum Fisher information of $\overline{\mathcal{N}}(\bar{\rho}(\boldsymbol{\theta}))$.

The Fisher-information analysis and optimal estimation strategy for this setting have been studied in Ref. [43], which we review in Appendix B. In particular, the optimal measurement basis (characterized by Eq. (9)) is the one that diagonalizes the target Pauli operator \bar{P}_i . Indeed, measuring $\overline{\mathcal{N}}(\bar{\rho}(\boldsymbol{\theta}))$ with \bar{P}_i yields the binary distribution

$$\Pr^{\text{L}}(x|\theta_i) = \frac{1 + x(1 - 2\epsilon_i)\theta_i}{2}, \quad (19)$$

where $x = \pm 1$ denotes the logical measurement outcome, and the superscript L indicates that the protocol is performed purely at the logical layer without using the error-syndrome record. As reviewed in Sec. II A, an asymptotically efficient estimator is given by the maximum-likelihood estimator in Eq. (3). In this specific binary-outcome setting, however, one can write down a simple optimal unbiased estimator explicitly. Given outcomes x_1, \dots, x_N obtained by measuring N copies of $\overline{\mathcal{N}}(\bar{\rho}(\boldsymbol{\theta}))$ with \bar{P}_i , an unbiased estimator can be constructed as

$$\theta_i^{\text{est}} = \frac{1}{N} \sum_{j=1}^N \frac{x_j}{(1 - 2\epsilon_i)}, \quad (20)$$

i.e., by averaging the rescaled outcomes $x_j/(1 - 2\epsilon_i)$. This estimator satisfies $\mathbb{E}[\theta_i^{\text{est}}] = \theta_i$ and has variance

$$\text{Var}[\theta_i^{\text{est}}] = \frac{1}{N} \frac{1 - (1 - 2\epsilon_i)^2 \theta_i^2}{(1 - 2\epsilon_i)^2}, \quad (21)$$

which attains the (quantum) Cramér–Rao bound in Eqs. (2), (8). This is because both the classical Fisher information $F_{\theta_i}^{\text{L}}$ of the probability distribution $\Pr^{\text{L}}(x|\theta_i)$ (defined in Eq. (1)) and the quantum Fisher information $J_{\theta_i}^{\text{L}}$ of the noisy logical state $\overline{\mathcal{N}}(\bar{\rho}(\boldsymbol{\theta}))$ for θ_i (defined in Eq. (7)) coincide and are given by

$$J_{\theta_i}^{\text{L}} = F_{\theta_i}^{\text{L}} = f_{\theta_i}(\epsilon_i) = f_{\theta_i} \left(\sum_{s \in \mathcal{S}} p_s \epsilon_{i,s} \right). \quad (22)$$

Here,

$$f_{\theta_i}(\epsilon_i) = \frac{(1 - 2\epsilon_i)^2}{1 - (1 - 2\epsilon_i)^2 \theta_i^2} \quad (23)$$

is a convex function of ϵ_i on $[0, 1/2]$. The equality $J_{\theta_i}^{\text{L}} = F_{\theta_i}^{\text{L}}$ implies that measuring \bar{P}_i is optimal in this setting. We provide a detailed derivation of the Fisher information in Appendix B.

In the following sections, we use the Fisher information of the syndrome-agnostic protocol, $J_{\theta_i}^{\text{L}} = F_{\theta_i}^{\text{L}} = f_{\theta_i}(\epsilon_i)$, as the baseline for comparison. In particular, for a classical (quantum) syndrome-aware protocol, we define its

effective logical error rate $\epsilon_i^{\text{cSynd}} (\epsilon_i^{\text{qSynd}})$ as the logical error rate such that $f_{\theta_i}(\epsilon_i^{\text{cSynd}}) (f_{\theta_i}(\epsilon_i^{\text{qSynd}}))$ matches the Fisher information achieved by that protocol. By comparing $\epsilon_i^{\text{cSynd}} (\epsilon_i^{\text{qSynd}})$ with the original logical error rate ϵ_i , we quantify how much the impact of noise can be reduced by incorporating error-syndrome information at the estimation stage.

V. FUNDAMENTAL LIMITATIONS ON CLASSICAL SYNDROME-AWARE PROTOCOLS

In this section, we study *classical* syndrome-aware estimation protocols, in which the logical measurement basis is fixed to \bar{P}_i regardless of the observed error syndrome s , and syndrome information is used only in classical post-processing (Fig. 2(b)). This class includes well-known protocols such as post-selection based on an estimated conditional logical error rate [19–25], as well as syndrome-conditioned variants of quantum error mitigation methods [9, 26–28] such as rescaling [18], zero-noise extrapolation [11, 14, 44] (since, in our model, the noise strength can be increased classically after measurement), probabilistic error cancellation [11, 45, 46] (since, in our model, noise inversion can be implemented by classically flipping measurement outcomes according to an appropriate quasiprobability distribution), symmetry verification [47, 48], and learning-based methods [49, 50].

Our analysis is based on the classical Fisher information of the outcome distribution obtained by measuring the syndrome-conditioned logical state with \bar{P}_i , together with the *effective logical error rate*, defined as the logical error rate of a syndrome-agnostic protocol that would yield the same classical Fisher information as a given classical syndrome-aware protocol. In Sec. V A, we derive the classical Fisher information and the corresponding effective logical error rate in our setup. In Sec. V B, we prove a universal lower bound on the effective logical error rate, showing that, on average, it cannot be smaller than one-half of the logical error rate. In Sec. V C, we further analyze the effective logical error rate, with particular emphasis on the low-error regime. Finally, in Sec. V D, we numerically investigate the effective logical error rate for several representative quantum error-correcting codes.

A. Classical Fisher information and effective logical error rate

As discussed in Sec. III, a syndrome-aware protocol is an estimation protocol performed on the classical-quantum state $\sum_{s \in \mathcal{S}} p_s |s\rangle\langle s| \otimes \overline{\mathcal{N}}_s(\bar{\rho}(\boldsymbol{\theta}))$. In particular, for the classical syndrome-aware protocol, the logical measurement applied to each syndrome-conditioned noisy logical state $\overline{\mathcal{N}}_s(\bar{\rho}(\boldsymbol{\theta}))$ is fixed to \bar{P}_i , which is the optimal measurement basis for the syndrome-agnostic protocol. Therefore, a classical syndrome-aware protocol can

be modeled as an estimation protocol based on the classical joint distribution

$$\Pr^{\text{Synd}}(x, s|\theta_i) = p_s \Pr^{\text{L}}(x|s, \theta_i), \quad (24)$$

where

$$\Pr^{\text{L}}(x|s, \theta_i) = \frac{1 + x(1 - 2\epsilon_{i,s})\theta_i}{2} \quad (25)$$

is the outcome distribution conditioned on the syndrome s . Equivalently, given N samples $(x_1, s_1), \dots, (x_N, s_N)$ drawn from $\Pr^{\text{Synd}}(x, s|\theta_i)$, the goal is to construct an unbiased estimator θ_i^{est} of θ_i . Hence, the ultimate precision and sampling overhead of classical syndrome-aware protocols can be analyzed via the classical Fisher information of $\Pr^{\text{Synd}}(x, s|\theta_i)$.

From Eq. (4) and Eq. (22), the classical Fisher information $F_{\theta_i}^{\text{Synd}}$ of $\Pr^{\text{Synd}}(x, s|\theta_i)$ is given by

$$F_{\theta_i}^{\text{Synd}} = \sum_{s \in \mathcal{S}} p_s f_{\theta_i}(\epsilon_{i,s}), \quad (26)$$

where the function $f_{\theta_i}(\epsilon)$ is defined in Eq. (23). Since $f_{\theta_i}(\epsilon)$ is convex in ϵ , Jensen's inequality implies

$$J_{\theta_i}^{\text{L}} = F_{\theta_i}^{\text{L}} \leq F_{\theta_i}^{\text{Synd}}. \quad (27)$$

In other words, the syndrome-aware distribution $\Pr^{\text{Synd}}(x, s|\theta_i)$ contains more information than the averaged logical distribution $\Pr^{\text{L}}(x|\theta_i) = \sum_s p_s \Pr^{\text{Synd}}(x, s|\theta_i)$. Thus, incorporating error-syndrome information can improve estimation accuracy (equivalently, reduce the required sampling overhead), compared to syndrome-agnostic estimation. In other words, the effective impact of logical noise can be reduced by exploiting the syndrome information.

To quantify this improvement, we define the *effective logical error rate* $\epsilon_i^{\text{cSynd}}$ for classical syndrome-aware estimation protocols by

$$f_{\theta_i}(\epsilon_i^{\text{cSynd}}) = F_{\theta_i}^{\text{Synd}} = \sum_{s \in \mathcal{S}} p_s f_{\theta_i}(\epsilon_{i,s}). \quad (28)$$

Equivalently, $\epsilon_i^{\text{cSynd}}$ is the logical error rate of a syndrome-agnostic protocol that would achieve the same Fisher information as the classical syndrome-aware protocol. By comparing $\epsilon_i^{\text{cSynd}}$ with the original logical error rate ϵ_i , we quantify how much the impact of noise can be reduced when incorporating error-syndrome information at the estimation stage.

We end this section by commenting on an asymptotically optimal classical syndrome-aware estimator that attains the Cramér–Rao bound in Eq. (2). Given N samples $(x_1, s_1), \dots, (x_N, s_N)$ from $\Pr^{\text{Synd}}(x, s|\theta_i)$, we first construct a rough initial unbiased estimator θ_i^{init} using the initial $N' = \lfloor \sqrt{N} \rfloor$ samples. Using the remaining $N - N'$ samples, we then define

$$\theta_i^{\text{est}} = \sum_{j=N'+1}^N \frac{f_{\theta_i^{\text{init}}}(\epsilon_{i,s_j})}{\sum_{j'=N'+1}^N f_{\theta_i^{\text{init}}}(\epsilon_{i,s_{j'}})} \frac{x_j}{(1 - 2\epsilon_{i,s_j})}. \quad (29)$$

This estimator can be regarded as a weighted average of the syndrome-agnostic estimator in Eq. (20), where the weights are proportional to the conditional Fisher informations $f_{\theta_i^{\text{init}}}(\epsilon_{i,s_j})$. In the asymptotic regime $N \rightarrow \infty$, we have $\theta_i^{\text{init}} \rightarrow \theta_i$ and $f_{\theta_i^{\text{init}}} \rightarrow f_{\theta_i}$, and moreover $\sum_{j=N'+1}^N f_{\theta_i}(\epsilon_{i,s_j}) \rightarrow N F_{\theta_i}^{\text{Synd}}$. Therefore, $\text{Var}(\theta_i^{\text{est}}) \rightarrow (N F_{\theta_i}^{\text{Synd}})^{-1}$, and the estimator attains the Cramér–Rao bound in Eq. (2). We note that a similar unbiased estimator was considered in Ref. [28], although its optimality was not discussed there.

B. Lower bounds on the effective logical error rate

As defined in the previous subsection, the effective logical error rate $\epsilon_i^{\text{cSynd}}$ quantifies the residual effect of errors inherent to classical syndrome-aware protocols. By analyzing how much $\epsilon_i^{\text{cSynd}}$ can be reduced relative to the original logical error rate ϵ_i , we can assess how much incorporating syndrome information can mitigate the impact of noise. However, as shown in the following theorem, $\epsilon_i^{\text{cSynd}}$ cannot be made arbitrarily small: it can improve over ϵ_i only by a constant factor.

Theorem 1. *The effective logical error rate $\epsilon_i^{\text{cSynd}}$ of classical syndrome-aware protocols satisfies*

$$\frac{1 - \theta_i^2}{2} \epsilon_i \leq \epsilon_i^{\text{cSynd}} \leq \epsilon_i, \quad (30)$$

where ϵ_i is the logical error rate under the maximum-likelihood decoder and $\theta_i = \text{tr}[\bar{P}_i \bar{\rho}(\boldsymbol{\theta})]$ is the expectation value to be estimated. In particular, when the ideal quantum state $\bar{\rho}(\boldsymbol{\theta}) = |\psi\rangle\langle\psi|$ is drawn from the k -qubit Haar measure, the average effective logical error rate satisfies

$$\frac{1}{2} \epsilon_i \lesssim \mathbb{E}_{\text{Haar}}[\epsilon_i^{\text{cSynd}}] \leq \epsilon_i, \quad (31)$$

where \lesssim indicates that the inequality holds up to the leading order in k .

We provide a proof of Theorem 1 in Appendix C1, which relies only on the convexity of the Fisher information function $f_{\theta_i}(\epsilon)$. A key point is that the bound is derived without assuming any specific code family or noise model. Therefore, within our setting of logical Pauli observable estimation, Theorem 1 is universal: $\epsilon_i^{\text{cSynd}}$ cannot be smaller than one half of the logical error rate ϵ_i achieved by the maximum-likelihood decoder on average, regardless of the code or the underlying noise model. We note that the assumption that we use the maximum-likelihood decoder is necessary to ensure $0 \leq \epsilon_{i,s} \leq 1/2$, so that the function $f_{\theta_i}(\epsilon_{i,s})$ is invertible on the domain $0 \leq \epsilon_{i,s} \leq 1/2$.

Several recent works report that post-selecting syndromes with low estimated error probability can reduce the logical error rate by orders of magnitude, lower the apparent threshold, and even allow a smaller

code distance [19–25]. At first glance, such observations might seem to contradict Theorem 1. However, these analyses focus on the *post-selected* logical error rate $\sum_{s \in \mathcal{S}^{\text{Post}}} p_s \epsilon_{i,s} / \sum_{s \in \mathcal{S}^{\text{Post}}} p_s$, where $\mathcal{S}^{\text{Post}} \subset \mathcal{S}$ is the set of error syndromes being post-selected, and typically do not account for the increased sampling overhead incurred by post-selection. Our result can be interpreted as follows: once the sampling overhead induced by post-selection is properly included, the net reduction of logical errors (as quantified by the effective logical error rate) is bounded by a constant factor, at most 1/2. Consequently, quantities such as the code distance or the threshold cannot be improved in an asymptotic sense solely by syndrome-dependent classical post-processing at the estimation stage. We formalize this intuition in the following corollary, whose proof is provided in appendix C 2.

Corollary 1. *Assume that $\theta_i \neq \pm 1$. Assume further that the logical error rate under the maximum-likelihood decoder scales as $\epsilon_i = \Theta(\eta^l)$ for some constant l , where η is a physical error rate. Then, the effective logical error rate of classical syndrome-aware protocols also scales as $\epsilon_i^{\text{cSynd}} = \Theta(\eta^l)$, i.e., the effective code distance does not change. Moreover, the threshold defined in terms of $\epsilon_i^{\text{cSynd}}$ is identical to that defined in terms of the logical error rate ϵ_i under the maximum-likelihood decoder.*

Using the lower bound on $\epsilon_i^{\text{cSynd}}$, we can also derive a lower bound on the sampling overhead for classical syndrome-aware estimation protocols. In quantum error mitigation, the sampling overhead is known to grow exponentially with the total error rate ϵ_{tot} of the circuit, typically as $e^{2\epsilon_{\text{tot}}}$ [18, 31]. This scaling also applies directly to syndrome-agnostic protocols when these results are applied to logical circuits. However, it has been unclear how much this overhead can be reduced by incorporating syndrome information. Theorem 1 provides a rigorous answer: even when syndrome information is used at the logical-layer estimation stage, the average effective logical error rate can improve by at most a factor of two. Accordingly, the sampling overhead can improve at best quadratically, reducing the scaling from $e^{2\epsilon_{\text{tot}}}$ to $e^{\epsilon_{\text{tot}}}$, and therefore the exponential overhead cannot be avoided. We state this formally as the following corollary.

Corollary 2. *The minimal sampling overhead for classical syndrome-aware protocols $N^{\text{cSynd}} = (\sigma_{\text{target}}^2 F_{\theta_i}^{\text{Synd}})^{-1}$ satisfies*

$$\frac{(1 - \theta_i^2)}{\sigma_{\text{target}}} \sqrt{N^{\text{L}} + \frac{\theta_i^2}{\sigma_{\text{target}}^2}} \leq N^{\text{cSynd}} \leq N^{\text{L}}, \quad (32)$$

where $N^{\text{L}} = (\sigma_{\text{target}}^2 F_{\theta_i}^{\text{L}})^{-1}$ is the minimal sampling overhead for syndrome-agnostic protocols and σ_{target} is the target standard deviation. In particular, when the ideal logical state is drawn from the k -qubit Haar measure, the average sampling overhead satisfies

$$\frac{1}{\sigma_{\text{target}}} \sqrt{\mathbb{E}_{\text{Haar}}[N^{\text{L}}]} \lesssim \mathbb{E}_{\text{Haar}}[N^{\text{cSynd}}] \leq \mathbb{E}_{\text{Haar}}[N^{\text{L}}]. \quad (33)$$

Here, the minimal sampling overhead in Corollary 2 is defined as the sample size N that attains equality in the Cramér–Rao bound in Eq. (2). Corollary 2 shows that N^{cSynd} can be at most quadratically smaller than the syndrome-agnostic overhead N^{L} . Since N^{L} grows exponentially with the total error rate as $e^{2\epsilon_{\text{tot}}}$ [18, 31], the exponential overhead in $N^{\text{cSynd}} = \Omega(e^{\epsilon_{\text{tot}}})$ cannot be avoided. We provide a proof of Corollary 2 in appendix C 3.

We emphasize that the fundamental limitations established here apply to a broad class of previously proposed classical syndrome-aware strategies, including post-selection based on syndrome records [19–25] and syndrome-conditioned variants of logical-layer quantum error mitigation [9, 26–28]. For instance, post-selection based on syndrome records can be viewed as using syndrome information to convert a subset of leading logical faults into detectable erasure events. When detecting such errors, the sampling overhead typically scales as $e^{p_{\text{tot}}}$ (as in symmetry verification [47, 48]), which is quadratically smaller than the generic quantum-error-mitigation overhead $e^{2p_{\text{tot}}}$ required to handle undetectable logical faults [18, 31]. Our Theorem 1 and Corollary 2 show that classical syndrome-aware protocols cannot yield a better scaling of the sampling overhead than the one achievable by such error-detection-based strategies. Our bounds are also consistent with numerical observations for syndrome-conditioned mitigation protocols. In particular, Ref. [28] reported that the blowup rate λ , defined from the sampling overhead $e^{\lambda p_{\text{tot}}}$ of given quantum error mitigation method (which is closely related to our effective logical error rate), is reduced by a factor no larger than 1/2, which is precisely explained by the universal limitation in Theorem 1.

C. Analysis in the low-error regime

In the previous subsections, we showed that exploiting syndrome information can reduce the effective impact of logical noise. Here, we analyze when such an error reduction is possible in the low-error regime. Specifically, we characterize when the effective logical error rate $\epsilon_i^{\text{cSynd}}$ can be strictly smaller than the logical error rate ϵ_i , i.e., when $\epsilon_i^{\text{cSynd}} < \epsilon_i$, in the limit of small physical noise.

We recall that the logical error rate ϵ_i can be written as a weighted average of the syndrome-conditioned logical error rates:

$$\epsilon_i = \sum_{s \in \mathcal{S}} p_s \epsilon_{i,s}. \quad (34)$$

Moreover, in the low-error regime, the effective logical error rate admits an expansion in terms of syndrome con-

tributions:

$$\begin{aligned}\epsilon_i^{\text{cSynd}} &\sim \frac{f_{\theta_i}(\epsilon_i^{\text{cSynd}}) - f_{\theta_i}(0)}{f_{\theta_i}^{(1)}} \\ &\sim \sum_{s \in \mathcal{S}} p_s \frac{f_{\theta_i}(\epsilon_{i,s}) - f_{\theta_i}(0)}{f_{\theta_i}^{(1)}}.\end{aligned}\quad (35)$$

Here, \sim means equality up to terms that are $o(\epsilon_i^{\text{cSynd}})$. To obtain the equality, we expand $f_{\theta_i}(\epsilon)$ around $\epsilon = 0$ as $f_{\theta_i}(\epsilon) = f_{\theta_i}(0) + f_{\theta_i}^{(1)}\epsilon + O(\epsilon^2)$, and use the definition of $\epsilon_i^{\text{cSynd}}$ in Eq. (28). Therefore, to analyze the (effective) logical error rate in the low-error regime, it suffices to understand the contribution of each syndrome individually.

We now identify which syndromes can affect the leading-order behavior. Consider an $[[n, k, d]]$ stabilizer code under a local noise model in which single-qubit Pauli errors occur independently on each physical qubit with probability η . We assume that the minimum weight of a logical Pauli operator that anti-commutes with the target logical Pauli operator \bar{P}_i is also d , so that $\epsilon_i = \Theta(\eta^{\lfloor (d+1)/2 \rfloor})$. Suppose a syndrome s occurs with probability $p_s = \Theta(\eta^l)$. Then, by the definition of code distance, the conditional logical error rate scales as $\epsilon_{i,s} = O(\eta^{\max\{d-2l, 0\}})$, and hence $p_s \epsilon_{i,s} = O(\eta^{\max\{d-l, l\}})$. On the other hand, the logical error rate and the effective logical error rate scale as $\epsilon_i, \epsilon_i^{\text{cSynd}} = \Theta(\eta^{\lfloor (d+1)/2 \rfloor})$ in the low-error regime. Therefore, syndromes with $p_s \epsilon_{i,s} = o(\eta^{\lfloor (d+1)/2 \rfloor})$ do not contribute to the leading-order term of ϵ_i or $\epsilon_i^{\text{cSynd}}$. Consequently, the dominant syndromes are those satisfying

$$p_s \epsilon_{i,s} = \Theta(\eta^{\lfloor (d+1)/2 \rfloor}). \quad (36)$$

In other words, $\max\{d-l, l\} = \lfloor (d+1)/2 \rfloor$, so we have $l = d/2$ when d is even and $l = (d-1)/2, (d+1)/2$ when d is odd. In the following, we analyze these dominant contributions separately depending on the parity of the code distance d .

1. When the code distance d is even

When the code distance d is even, the condition $p_s \epsilon_{i,s} = \Theta(\eta^{\lfloor (d+1)/2 \rfloor}) = \Theta(\eta^{d/2})$ is satisfied by syndromes for which $l = d/2$, i.e., $p_s = \Theta(\eta^{d/2}) = \Theta(\epsilon_i)$ and $\epsilon_{i,s} = \Theta(1)$. Since the syndrome-conditioned logical error rate remains $\Theta(1)$ for such syndromes, we denote the set of these syndromes by $\mathcal{S}_{\Theta(1)} \subset \mathcal{S}$. Then,

$$\begin{aligned}\epsilon_i &\sim \sum_{s \in \mathcal{S}_{\Theta(1)}} p_s \epsilon_{i,s}, \\ \epsilon_i^{\text{cSynd}} &\sim \sum_{s \in \mathcal{S}_{\Theta(1)}} p_s \frac{f_{\theta_i}(\epsilon_{i,s}) - f_{\theta_i}(0)}{f_{\theta_i}^{(1)}},\end{aligned}\quad (37)$$

where \sim means equality up to terms that are $o(\eta^{d/2})$.

For $s \in \mathcal{S}_{\Theta(1)}$, the conditional logical error rate does not vanish as the physical error rate η decreases, but instead converges to a constant, i.e., $\epsilon_{i,s} = \Theta(1)$. Operationally, observing such a syndrome indicates a persistent decoding ambiguity: there exist at least two error configurations of the same weight of $d/2$ that induce different logical actions. In syndrome-agnostic protocols, the contributions of these ambiguous syndromes $s \in \mathcal{S}_{\Theta(1)}$ are inseparable, because the syndrome record is discarded. In contrast, syndrome-aware protocols can apply different classical post-processing conditioned on $s \in \mathcal{S}_{\Theta(1)}$, which can improve the effective logical error rate. Indeed, for any fixed $\epsilon_{i,s} = \Theta(1) > 0$, we have $(f_{\theta_i}(\epsilon_{i,s}) - f_{\theta_i}(0))/f_{\theta_i}^{(1)} < \epsilon_{i,s}$ from the convexity of the function $f_{\theta_i}(\epsilon)$, so that $\epsilon_i^{\text{cSynd}}$ becomes strictly smaller than ϵ_i in the low-error regime. Because such ambiguous syndromes $s \in \mathcal{S}_{\Theta(1)}$ always exist when d is even, $\epsilon_i^{\text{cSynd}}$ is always strictly smaller than ϵ_i as $\eta \rightarrow 0$:

Proposition 1. *When the code distance d is even, the effective logical error rate $\epsilon_i^{\text{cSynd}}$ is strictly smaller than the logical error rate ϵ_i under the maximum-likelihood decoder in the limit $\eta \rightarrow 0$:*

$$\frac{1 - \theta_i^2}{2} \leq \lim_{\eta \rightarrow 0} \frac{\epsilon_i^{\text{cSynd}}}{\epsilon_i} < 1. \quad (38)$$

The equality for $(1 - \theta_i^2)/2$ is achieved if and only if $\epsilon_{i,s} = 1/2$ for all $s \in \mathcal{S}_{\Theta(1)}$.

We provide a proof of Proposition 1 in Appendix C 4. The strict inequality $\lim_{\eta \rightarrow 0} \epsilon_i^{\text{cSynd}}/\epsilon_i < 1$ means that, for even-distance codes, syndrome-aware classical post-processing always yields a nontrivial improvement in the small-error regime. This occurs because ambiguous syndromes $s \in \mathcal{S}_{\Theta(1)}$, for which a finite conditional logical error persists, necessarily appear when d is even. Moreover, when the decoding ambiguity is maximal, i.e., $\epsilon_{i,s} = 1/2$ for all $s \in \mathcal{S}_{\Theta(1)}$, the improvement from using syndrome information is maximized, and the lower bound in Theorem 1 can be achieved. An example is the distance-2 rotated surface code with parameters $[[4, 1, 2]]$.

2. When the code distance d is odd

When the code distance d is odd, the syndromes satisfying $p_s \epsilon_{i,s} = \Theta(\eta^{\lfloor (d+1)/2 \rfloor}) = \Theta(\eta^{(d+1)/2})$ can be classified into two classes corresponding to $l = (d+1)/2$ and $l = (d-1)/2$ in $p_s = \Theta(\eta^l)$: those with $p_s = \Theta(\eta^{(d+1)/2}) = \Theta(\epsilon_i)$ and conditional logical error rate $\epsilon_{i,s} = \Theta(1)$, and those with $p_s = \Theta(\eta^{(d-1)/2}) = \Theta(\epsilon_i/\eta)$ and conditional logical error rate $\epsilon_{i,s} = \Theta(\eta)$. We denote the former set by $\mathcal{S}_{\Theta(1)} \subset \mathcal{S}$ and the latter by $\mathcal{S}_{\Theta(\eta)} \subset \mathcal{S}$. Unlike the even-distance case, the syndromes $s \in \mathcal{S}_{\Theta(\eta)}$ with $\epsilon_{i,s} = \Theta(\eta)$ also contribute to the leading-order terms of the (effective) logical error rates ϵ_i and $\epsilon_i^{\text{cSynd}}$. However, since these syndromes have vanishing

conditional logical error rate in the limit $\eta \rightarrow 0$, they do not lead to an improvement from syndrome awareness. Indeed, for $s \in \mathcal{S}_{\Theta(\eta)}$ we have $(f_{\theta_i}(\epsilon_{i,s}) - f_{\theta_i}(0))/f_{\theta_i}^{(1)} = \epsilon_{i,s} + O(\epsilon_{i,s}^2)$, so their contributions to $\epsilon_i^{\text{cSynd}}$ coincide with those to ϵ_i at leading order. Therefore,

$$\begin{aligned} \epsilon_i &\sim \sum_{s \in \mathcal{S}_{\Theta(\eta)}} p_s \epsilon_{i,s} + \sum_{s \in \mathcal{S}_{\Theta(1)}} p_s \epsilon_{i,s}, \\ \epsilon_i^{\text{cSynd}} &\sim \sum_{s \in \mathcal{S}_{\Theta(\eta)}} p_s \epsilon_{i,s} + \sum_{s \in \mathcal{S}_{\Theta(1)}} p_s \frac{f_{\theta_i}(\epsilon_{i,s}) - f_{\theta_i}(0)}{f_{\theta_i}^{(1)}}, \end{aligned} \quad (39)$$

where \sim denotes equality up to terms that are $o(\eta^{(d+1)/2})$. In other words, only the ambiguous syndromes $s \in \mathcal{S}_{\Theta(1)}$ with non-vanishing conditional logical error are responsible for any improvement. However, such syndromes $s \in \mathcal{S}_{\Theta(1)}$ do not necessarily exist for odd-distance codes. Therefore, an improvement from using syndrome information at the logical estimation stage is not guaranteed in general. In fact, we obtain the following proposition.

Proposition 2. *When the code distance d is odd, the effective logical error rate $\epsilon_i^{\text{cSynd}}$ is strictly smaller than the logical error rate ϵ_i under the maximum-likelihood decoder only if $\mathcal{S}_{\Theta(1)} \neq \emptyset$. Equivalently,*

$$\lim_{\eta \rightarrow 0} \frac{\epsilon_i^{\text{cSynd}}}{\epsilon_i} < 1 \quad (40)$$

holds if and only if $\mathcal{S}_{\Theta(1)} \neq \emptyset$; otherwise, $\lim_{\eta \rightarrow 0} \epsilon_i^{\text{cSynd}}/\epsilon_i = 1$.

We provide the proof of Proposition 2 in Appendix C5. Proposition 2 gives a sharp criterion for when classical syndrome awareness yields a nontrivial improvement in the low-error regime $\eta \rightarrow 0$: $\epsilon_i^{\text{cSynd}} < \epsilon_i$ holds if and only if $\mathcal{S}_{\Theta(1)} \neq \emptyset$. Most odd-distance quantum codes, including the Steane code and odd-distance rotated surface codes, satisfy this condition. Meanwhile, the $[[5, 1, 3]]$ perfect code does not satisfy this condition because all error syndromes occur with $p_s = O(1)$ or $p_s = O(\eta)$, and thus $\epsilon_{i,s} = O(\eta^2)$ or $\epsilon_{i,s} = O(\eta)$. Therefore, we cannot obtain an advantage for such a code.

Another important example that violates the condition in Proposition 2 arises when decoding bit-flip errors in CSS codes, especially when an arbitrary X -type logical observable has odd weight. In CSS codes, it is common to decode bit-flip errors using only Z -type stabilizer measurements. Under such a decoding strategy, we have $\mathcal{S}_{\Theta(1)} = \emptyset$ whenever an arbitrary X -type logical observable has odd weight. This is because $\mathcal{S}_{\Theta(1)} \neq \emptyset$ would imply the existence of syndromes occurring with $p_s = \Theta(\eta^{(d+1)/2})$ and having conditional logical error rate $\epsilon_{i,s} = \Theta(1)$. Equivalently, there must exist two distinct weight- $(d+1)/2$ bit-flip errors that induce different logical actions, which in turn would require the existence of an even-distance X -type logical operator. Examples

exhibiting this behavior include the $[[7, 1, 3]]$ Steane code and odd-distance rotated surface codes. This means that whether the effective logical error rate $\epsilon_i^{\text{cSynd}}$ is strictly smaller than the original logical error rate ϵ_i depends on the decoding strategy: even though we can obtain an advantage of using the error syndrome when decoding using both X -type and Z -type stabilizer measurements, the advantage is lost when we restrict to using only Z -type stabilizer measurements.

D. Numerical analysis

In this subsection, we numerically evaluate the improvement achievable by classical syndrome-aware protocols for several representative quantum error-correcting codes. Specifically, we compute the ratio of the effective logical error rate $\epsilon_i^{\text{cSynd}}$ to the logical error rate ϵ_i under the maximum-likelihood decoder. We consider the $[[4, 1, 2]]$ rotated surface code, the $[[5, 1, 3]]$ perfect code, the $[[7, 1, 3]]$ Steane code, the $[[9, 1, 3]]$ rotated surface code, and the $[[12, 2, 4]]$ carbon code [51]. As a noise model, we assume local depolarizing noise acting independently on each physical qubit with physical error rate η . We take the target observable \bar{P}_i to be the logical Pauli- Z operator on the first logical qubit and set $\theta_i = 0$. For CSS codes, we additionally consider a restricted decoding strategy in which bit-flip errors are decoded using only the syndrome outcomes of Z -type stabilizer generators.

The results are shown in Fig. 3. For all codes, we confirm that the ratio $\epsilon_i^{\text{cSynd}}/\epsilon_i$ satisfies the universal bounds established in Theorem 1. We also observe a qualitative difference between even- and odd-distance codes, consistent with the discussion in Sec. VC. For even-distance codes, the dominant contribution to the (effective) logical error rate arises from ambiguous syndromes $s \in \mathcal{S}_{\Theta(1)}$ with non-vanishing conditional logical error probabilities, whose impact can be reduced by syndrome-aware classical post-processing at the estimation stage. Accordingly, the ratio approaches a value close to the lower bound in Theorem 1. Moreover, for the $[[4, 1, 2]]$ rotated surface code, we have $\epsilon_{i,s} = 1/2$ for all $s \in \mathcal{S}_{\Theta(1)}$, and thus the lower bound is attained, as discussed in Proposition 1.

By contrast, for odd-distance codes, syndromes $s \in \mathcal{S}_{\Theta(\eta)}$ with vanishing conditional logical error probabilities can also contribute at leading order to ϵ_i and $\epsilon_i^{\text{cSynd}}$, and their impact cannot be reduced by syndrome-aware classical post-processing. As a result, the ratio $\epsilon_i^{\text{cSynd}}/\epsilon_i$ for odd-distance codes is typically larger than that for even-distance codes. In particular, for the $[[5, 1, 3]]$ perfect code, we have $\mathcal{S}_{\Theta(1)} = \emptyset$ because the code is non-degenerate, and correspondingly we observe $\epsilon_i^{\text{cSynd}}/\epsilon_i \rightarrow 1$, in agreement with Proposition 2. Moreover, under the restricted decoding strategy that uses only Z -type stabilizer generators, the ratios also approach unity for the $[[7, 1, 3]]$ Steane code and the $[[9, 1, 3]]$ rotated surface

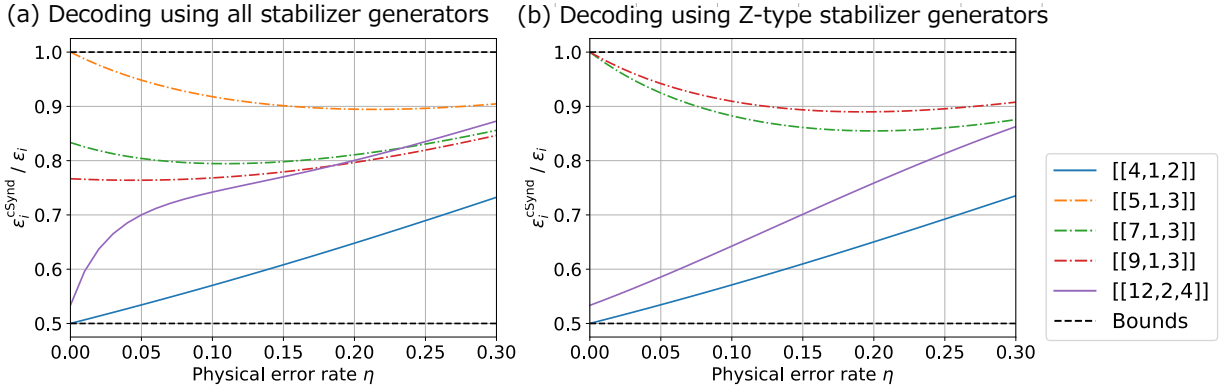


FIG. 3. Ratio $\epsilon_i^{\text{cSynd}}/\epsilon_i$ as a function of the physical error rate η for several stabilizer codes, where ϵ_i is the logical error rate under the maximum-likelihood decoder and $\epsilon_i^{\text{cSynd}}$ is the effective logical error rate of classical syndrome-aware protocols. We consider the $[[4,1,2]]$ rotated surface code, $[[5,1,3]]$ perfect code, $[[7,1,3]]$ Steane code, $[[9,1,3]]$ rotated surface code, and $[[12,2,4]]$ carbon code [51]. Solid (dash-dotted) lines correspond to even-distance (odd-distance) codes, and dashed lines indicate the universal bounds $(1 - \theta_i^2)/2 \leq \epsilon_i^{\text{cSynd}}/\epsilon_i \leq 1$ from Theorem 1, evaluated at $\theta_i = 0$. (a) Results obtained using syndrome outcomes from all stabilizer generators. (b) Results obtained when only syndrome outcomes from Z -type stabilizer generators are used to correct bit-flip errors. Note that the $[[5,1,3]]$ perfect code is not shown in this figure, since it is not a CSS code.

code, as discussed in Sec. V C.

So far, we have mainly focused on analyses based on the maximum-likelihood decoder, which is required to ensure the assumption $\epsilon_{i,s} \leq 1/2$ for all $s \in \mathcal{S}$. However, performing maximum-likelihood decoding—i.e., finding an optimal recovery operation for each syndrome $s \in \mathcal{S}$ —is known to be $\#P$ -hard [40, 41]. Moreover, to implement the optimal classical syndrome-aware protocol in Eq. (29), one needs to learn or calculate the syndrome-conditioned logical error rates $\epsilon_{i,s}$, whose number may grow exponentially with the code size n . For these reasons, the optimal syndrome-agnostic protocols (based on maximum-likelihood decoding) and the optimal classical syndrome-aware protocols (based on learning an exponential number of conditional logical error rates), which form the basis of our theoretical framework, may require excessive resource for actual experiments.

In practice, one instead employs decoders such as minimum-weight perfect matching [52, 53] or belief-propagation decoders followed by post-processing [54–57]. In such cases, because the decoder may fail to identify the optimal recovery for some syndromes, one can have $\epsilon_{i,s} > 1/2$ for certain $s \in \mathcal{S}$. Furthermore, rather than applying syndrome-dependent post-processing separately for all $s \in \mathcal{S}$, one may coarse-grain the syndrome space by partitioning it into M disjoint subsets as $\mathcal{S} = \bigsqcup_{j=1}^M \mathcal{S}_j$, and perform syndrome-aware estimation based only on which group \mathcal{S}_j contains the observed syndrome s . In this setting, the syndrome-aware protocol is modeled as an estimation procedure on the classical-quantum state

$$\sum_{j=1}^M p_{\mathcal{S}_j} |\mathcal{S}_j\rangle\langle\mathcal{S}_j| \otimes \bar{\mathcal{N}}_{\mathcal{S}_j}(\bar{\rho}(\theta)), \quad (41)$$

where $p_{\mathcal{S}_j} = \sum_{s \in \mathcal{S}_j} p_s$ is the probability of observing a syndrome in \mathcal{S}_j , $\{|\mathcal{S}_j\rangle\}_{j=1}^M$ is an orthonormal basis of a classical register representing the coarse-grained syndrome outcomes, and $\bar{\mathcal{N}}_{\mathcal{S}_j} = \sum_{s \in \mathcal{S}_j} p_s \bar{\mathcal{N}}_s / p_{\mathcal{S}_j}$ is the \mathcal{S}_j -conditioned logical noise channel. For the classical protocol, this corresponds to estimation based on the joint distribution

$$\Pr^{\text{Synd}}(x, \mathcal{S}_j | \theta_i) = p_{\mathcal{S}_j} \Pr^L(x | \mathcal{S}_j, \theta_i), \quad (42)$$

where

$$\Pr^L(x | \mathcal{S}_j, \theta_i) = \frac{1 + x(1 - 2\epsilon_{i,\mathcal{S}_j})\theta_i}{2} \quad (43)$$

is the outcome distribution conditioned on the group \mathcal{S}_j , and $\epsilon_{i,\mathcal{S}_j} = \sum_{s \in \mathcal{S}_j} p_s \epsilon_{i,s} / p_{\mathcal{S}_j}$ is the corresponding conditional logical error rate. By choosing the number of groups M to be tractable, one can estimate all $\epsilon_{i,\mathcal{S}_j}$ in advance and perform syndrome-aware estimation with reasonable computational cost.

We now evaluate the effectiveness of such practical syndrome-aware protocols. We consider the rotated surface code $[[d^2, 1, d]]$ for various distances d and decode using minimum-weight perfect matching. As a noise model, we assume local depolarizing noise acting independently on each physical qubit with physical error rate η . We take the target observable \bar{P}_i to be the logical Pauli- Z operator and set $\theta_i = 0$. We decode bit-flip errors using only the syndrome outcomes of Z -type stabilizer generators. We then coarse-grain syndromes according to the complementary gap [19–22, 58] as $\mathcal{S} = \bigsqcup_{j=1}^M \mathcal{S}_j$, where \mathcal{S}_j denotes the set of syndromes with the same complementary gap, and apply classical post-processing conditioned on this label, which is modeled by Eq. (42). We use Stim [59] and PyMatching [60] for the simulation.

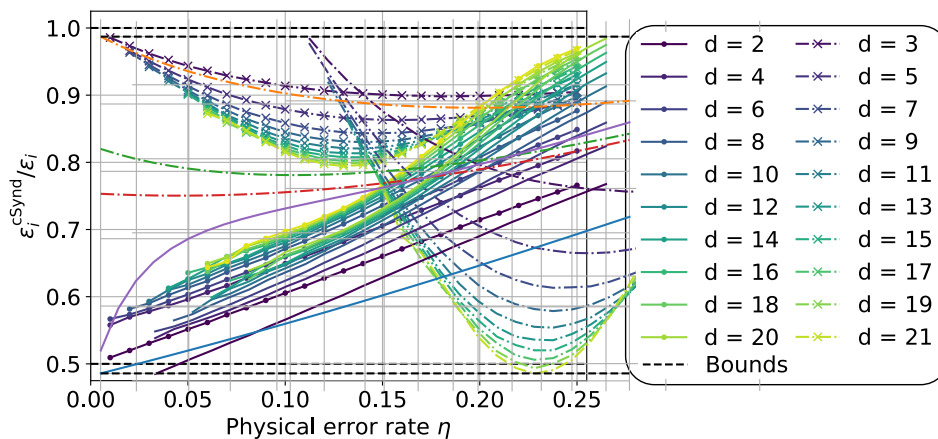


FIG. 4. Ratio $\epsilon_i^{cSynd}/\epsilon_i$ as a function of the physical error rate η for rotated surface codes, where ϵ_i is the logical error rate under the minimum-weight perfect matching decoder and ϵ_i^{cSynd} is the effective logical error rate of classical syndrome-aware protocols conditioned on the complementary gap. Solid (dash-dotted) lines correspond to even-distance (odd-distance) codes, and dashed lines indicate the universal bounds $(1 - \theta_i^2)/2 \leq \epsilon_i^{cSynd}/\epsilon_i \leq 1$ from Theorem 1, evaluated at $\theta_i = 0$.

In Fig. 4, we plot the ratio between the logical error rate ϵ_i under minimum-weight perfect matching and the effective logical error rate ϵ_i^{cSynd} defined via Eq. (42). Because the group-conditioned logical error rates ϵ_{i,S_j} can exceed $1/2$, the assumptions underlying Theorem 1 and Propositions 1–2 do not necessarily hold a priori. Nevertheless, we observe numerically that the same qualitative conclusions persist in this practical scenario. In particular, the ratio $\epsilon_i^{cSynd}/\epsilon_i$ never drops below $1/2$; for even-distance codes, we consistently obtain an improvement $\epsilon_i^{cSynd}/\epsilon_i < 1$ in the low-error regime; and for odd-distance codes, the ratio approaches 1, indicating no improvement in the low-error regime from using syndrome information at the logical estimation stage. Therefore, we conclude that our theoretical results are likely to hold even for such practical setups.

VI. EXPONENTIAL ADVANTAGES IN QUANTUM SYNDROME-AWARE PROTOCOLS

In this section, we turn to *quantum* syndrome-aware estimation protocols, in which syndrome-conditioned logical measurement can be tailored to the observed syndrome (Fig. 2(c)). That is, after observing the error syndrome s , one may choose a syndrome-dependent logical measurement basis before extracting classical data. This additional adaptivity fundamentally changes the information extractable from logical measurements and allows one to surpass the constant-factor limitations for classical syndrome-aware protocols established in Theorem 1.

Our analysis is based on the quantum Fisher information of the classical–quantum state $\sum_s p_s |s\rangle\langle s| \otimes \bar{\mathcal{N}}_s(\bar{\rho}(\boldsymbol{\theta}))$, defined in Eq. (16). Analogously to the classical case, we define the *effective logical error rate* ϵ_i^{qSynd} of a quantum syndrome-aware protocol as the logical er-

ror rate such that the syndrome-agnostic Fisher information $f_{\theta_i}(\epsilon_i^{qSynd})$ matches the quantum Fisher information of the classical–quantum state. In Sec. VIA, we derive the quantum Fisher information and the corresponding effective logical error rate in our setup. In Sec. VIB, we show that the effective logical error rate can be exponentially smaller than the logical error rate, yielding an exponential separation between classical and quantum syndrome-aware protocols. In Sec. VIC, we discuss an optimal estimation scheme that achieves the exponential advantage. Finally, in Sec. VID, we numerically investigate the generality of our results.

A. Quantum Fisher information and effective logical error rate

As discussed in Sec. III, a syndrome-aware estimation protocol acts on the classical–quantum state $\sum_s p_s |s\rangle\langle s| \otimes \bar{\mathcal{N}}_s(\bar{\rho}(\boldsymbol{\theta}))$, defined in Eq. (16). In quantum syndrome-aware protocols, unlike the classical case, one is allowed to perform arbitrary quantum measurement on the classical–quantum state. Accordingly, the quantum syndrome-aware estimation protocols can be modeled as, given N copies of $\sum_s p_s |s\rangle\langle s| \otimes \bar{\mathcal{N}}_s(\bar{\rho}(\boldsymbol{\theta}))$, constructing an unbiased estimator θ_i^{est} of θ_i . Thus, the ultimate precision and sampling overhead of quantum syndrome-aware protocols are characterized by the quantum Fisher information of this classical–quantum state.

Let us define the covariance matrix $C(\boldsymbol{\theta})$ of the ideal logical state $\bar{\rho}(\boldsymbol{\theta})$ by

$$C(\boldsymbol{\theta})_{ij} = \text{tr} \left[\bar{\rho}(\boldsymbol{\theta}) \frac{1}{2} \{ \bar{P}_i, \bar{P}_j \} \right] - \text{tr} [\bar{\rho}(\boldsymbol{\theta}) \bar{P}_i] \text{tr} [\bar{\rho}(\boldsymbol{\theta}) \bar{P}_j]. \quad (44)$$

Using $C(\boldsymbol{\theta})$, the quantum Fisher information matrix associated with the syndrome-conditioned noisy logical

state $\overline{\mathcal{N}}_s(\bar{\rho}(\boldsymbol{\theta}))$ can be written as $\Lambda_s C(\Lambda_s \boldsymbol{\theta})^{-1} \Lambda_s$ (see Appendix B or Ref. [43] for the derivation). Here, $\Lambda_s = \text{diag}(1 - 2\epsilon_{1,s}, \dots, 1 - 2\epsilon_{4^k-1,s})$ is a $(4^k - 1)$ -dimensional diagonal matrix describing the action of $\overline{\mathcal{N}}_s$ on the generalized Bloch vector, i.e., $\overline{\mathcal{N}}_s(\bar{\rho}(\boldsymbol{\theta})) = \bar{\rho}(\Lambda_s \boldsymbol{\theta})$. Therefore, from Eq. (12), the quantum Fisher information matrix for the classical-quantum state $\sum_s p_s |s\rangle\langle s| \otimes \overline{\mathcal{N}}_s(\bar{\rho}(\boldsymbol{\theta}))$ is

$$J^{\text{Synd}} = \sum_{s \in \mathcal{S}} p_s \Lambda_s C(\Lambda_s \boldsymbol{\theta})^{-1} \Lambda_s. \quad (45)$$

In particular, the quantum Fisher information for the parameter θ_i is

$$J_{\theta_i}^{\text{Synd}} = \frac{1}{\mathbf{e}_i^T (\sum_{s \in \mathcal{S}} p_s \Lambda_s C(\Lambda_s \boldsymbol{\theta})^{-1} \Lambda_s)^{-1} \mathbf{e}_i}, \quad (46)$$

where $\mathbf{e}_i \in \mathbb{R}^{4^k-1}$ is a unit vector whose j -th element is 1 if $j = i$ and 0 otherwise. From the monotonicity of the quantum Fisher information matrix (equivalently, since the quantum Fisher information is the maximum Fisher information over all measurements, and restricting the measurement basis cannot increase the Fisher information), we obtain

$$J_{\theta_i}^L = F_{\theta_i}^L \leq F_{\theta_i}^{\text{Synd}} \leq J_{\theta_i}^{\text{Synd}}. \quad (47)$$

This shows that allowing syndrome-conditioned quantum measurement can improve estimation accuracy (equivalently, reduce the required sampling overhead) compared to syndrome-agnostic and classical syndrome-aware protocols. In other words, the effective impact of logical noise can be reduced by exploiting syndrome-conditioned quantum measurement.

To quantify this improvement, we define the *effective logical error rate* $\epsilon_i^{\text{qSynd}}$ for quantum syndrome-aware protocols by

$$f_{\theta_i}(\epsilon_i^{\text{qSynd}}) = J_{\theta_i}^{\text{Synd}}. \quad (48)$$

Equivalently, $\epsilon_i^{\text{qSynd}}$ is the logical error rate of a syndrome-agnostic protocol that would achieve the same quantum Fisher information as the quantum syndrome-aware protocol. By comparing $\epsilon_i^{\text{qSynd}}$ with the original logical error rate ϵ_i , we quantify how much the impact of noise can be reduced by allowing syndrome-conditioned quantum measurement.

B. Exponential reduction in the effective logical error rate

As defined in the previous subsection, the effective logical error rate $\epsilon_i^{\text{qSynd}}$ quantifies the residual effect of errors inherent to quantum syndrome-aware protocols. By analyzing how much $\epsilon_i^{\text{qSynd}}$ can be reduced relative to the original logical error rate ϵ_i , we can assess how incorporating syndrome information at the logical measurement stage mitigates the impact of noise. In the classical case, Theorem 1 established a universal lower bound

showing that the effective logical error rate $\epsilon_i^{\text{cSynd}}$ can improve over ϵ_i only by a constant factor. In contrast, once syndrome-conditioned quantum measurement is allowed, such a limitation no longer holds, and $\epsilon_i^{\text{qSynd}}$ can be reduced exponentially with the number of logical qubits.

For a quantitative analysis, we consider the low-error regime, as in Sec. V C. Consider an $[[n, k, d]]$ stabilizer code under a local noise model in which single-qubit Pauli errors occur independently on each physical qubit with probability η . We assume that the minimum weight of a logical Pauli operator that anti-commutes with the target logical Pauli operator \bar{P}_i is also d , so that $\epsilon_i = \Theta(\eta^{\lfloor (d+1)/2 \rfloor})$. In the low-error regime, we can expand the effective logical error rate $\epsilon_i^{\text{qSynd}}$ in terms of syndrome contributions as

$$\begin{aligned} \epsilon_i^{\text{qSynd}} &\sim \frac{f_{\theta_i}(\epsilon_i^{\text{qSynd}})^{-1} - f_{\theta_i}(0)^{-1}}{4} \\ &= \frac{\mathbf{e}_i^T (\sum_{s \in \mathcal{S}} p_s \Lambda_s C(\Lambda_s \boldsymbol{\theta})^{-1} \Lambda_s)^{-1} \mathbf{e}_i - \mathbf{e}_i^T C(\boldsymbol{\theta}) \mathbf{e}_i}{4} \\ &\sim \sum_{s \in \mathcal{S}} p_s \Delta_i(\overline{\mathcal{N}}_s). \end{aligned} \quad (49)$$

Here, \sim denotes equality up to terms that are $o(\epsilon_i^{\text{qSynd}}) = o(\epsilon_i) = o(\eta^{\lfloor (d+1)/2 \rfloor})$, and

$$\Delta_i(\overline{\mathcal{N}}_s) = \frac{\mathbf{e}_i^T (C(\boldsymbol{\theta}) - C(\boldsymbol{\theta}) \Lambda_s C(\Lambda_s \boldsymbol{\theta})^{-1} \Lambda_s C(\boldsymbol{\theta})) \mathbf{e}_i}{4} \quad (50)$$

represents the contribution from syndrome s . To obtain the first relation in Eq. (49), we use $f_{\theta_i}(\epsilon)^{-1} = (1 - 2\epsilon)^{-2} - \theta_i^2 = 1 - \theta_i^2 + 4\epsilon + O(\epsilon^2)$. For the second relation, we use the definition of the effective logical error rate in Eq. (48), together with $f_{\theta_i}(0)^{-1} = 1 - \theta_i^2 = \mathbf{e}_i^T C(\boldsymbol{\theta}) \mathbf{e}_i$. For the third relation, we use $\sum_s p_s \Lambda_s C(\Lambda_s \boldsymbol{\theta})^{-1} \Lambda_s - C(\boldsymbol{\theta})^{-1} = O(\epsilon_i)$ and the expansion $(A + B)^{-1} \sim A^{-1} - A^{-1} B A^{-1}$ for square matrices A and B when $A \gg B$.

As in the classical case, the low-error behavior of ϵ_i and $\epsilon_i^{\text{qSynd}}$ depends on the parity of the distance d . Suppose a syndrome s occurs with probability $p_s = \Theta(\eta^l)$. Then, by the definition of code distance, the conditional logical error rate scales as $\epsilon_{i,s} = O(\eta^{\max\{d-2l, 0\}})$, and hence $p_s \epsilon_{i,s} = O(\eta^{\max\{d-l, l\}})$. Note that we also have $p_s \Delta_i(\overline{\mathcal{N}}_s) = O(\eta^{\max\{d-l, l\}})$. On the other hand, in the low-error regime we have $\epsilon_i, \epsilon_i^{\text{qSynd}} = \Theta(\eta^{\lfloor (d+1)/2 \rfloor})$. Therefore, syndromes with $p_s \epsilon_{i,s} = o(\eta^{\lfloor (d+1)/2 \rfloor})$ do not contribute to the leading-order term of either ϵ_i or $\epsilon_i^{\text{qSynd}}$. Consequently, the dominant syndromes are those satisfying

$$p_s \epsilon_{i,s} = O(\eta^{\max\{d-l, l\}}) = \Theta(\eta^{\lfloor (d+1)/2 \rfloor}), \quad (51)$$

which can be characterized as follows.

- When d is even: Syndromes s with $l = d/2$, i.e., $p_s = \Theta(\eta^{d/2}) = \Theta(\epsilon_i)$ and $\epsilon_{i,s} = \Theta(1)$ (denoted by

$\mathcal{S}_{\Theta(1)}$). The dominant terms can be written as

$$\begin{aligned}\epsilon_i &\sim \sum_{s \in \mathcal{S}_{\Theta(1)}} p_s \epsilon_{i,s}, \\ \epsilon_i^{\text{qSynd}} &\sim \sum_{s \in \mathcal{S}_{\Theta(1)}} p_s \Delta_i(\overline{\mathcal{N}}_s),\end{aligned}\quad (52)$$

up to terms of order $o(\eta^{\lfloor (d+1)/2 \rfloor})$.

- When d is odd: There are two types of dominant syndromes: (i) s with $l = (d+1)/2$, i.e., $p_s = \Theta(\eta^{(d+1)/2}) = \Theta(\epsilon_i)$ and $\epsilon_{i,s} = \Theta(1)$ (again denoted by $\mathcal{S}_{\Theta(1)}$), and (ii) s with $l = (d-1)/2$, i.e., $p_s = \Theta(\eta^{(d-1)/2}) = \Theta(\epsilon_i/\eta)$ and $\epsilon_{i,s} = \Theta(\eta)$ (denoted by $\mathcal{S}_{\Theta(\eta)}$). The dominant terms can be written as

$$\begin{aligned}\epsilon_i &\sim \sum_{s \in \mathcal{S}_{\Theta(\eta)}} p_s \epsilon_{i,s} + \sum_{s \in \mathcal{S}_{\Theta(1)}} p_s \epsilon_{i,s}, \\ \epsilon_i^{\text{qSynd}} &\sim \sum_{s \in \mathcal{S}_{\Theta(\eta)}} p_s \epsilon_{i,s} + \sum_{s \in \mathcal{S}_{\Theta(1)}} p_s \Delta_i(\overline{\mathcal{N}}_s).\end{aligned}\quad (53)$$

Here, we use $p_s \Delta_i(\overline{\mathcal{N}}_s) = p_s(\epsilon_{i,s} + O(\epsilon_{i,s}^2)) = p_s \epsilon_{i,s} + o(\eta^{(d+1)/2})$ for $s \in \mathcal{S}_{\Theta(\eta)}$.

As in the classical case, we see that error syndromes with non-vanishing conditional logical error rates, $s \in \mathcal{S}_{\Theta(1)}$, are responsible for the improvement in syndrome-aware protocols. In particular, when the conditional noise channel \mathcal{N}_s satisfies the following property, the contribution $\Delta_i(\overline{\mathcal{N}}_s)$ of such a syndrome s to the effective logical error rate $\epsilon_i^{\text{qSynd}}$ becomes exponentially small:

Lemma 1. *Let s be an error syndrome of an $[[n, k, d]]$ stabilizer code such that the conditional noise channel \mathcal{N}_s is represented as $\mathcal{N}_s(\cdot) = \frac{1}{2} \cdot + \frac{1}{2} \overline{Q} \cdot \overline{Q}$, where logical Pauli- \overline{Q} operator that anti-commutes with the target logical operator \overline{P}_i is applied with probability $1/2$. Then, when the ideal logical quantum state $\overline{\rho}(\theta) = |\psi\rangle\langle\psi|$ is drawn from the k -qubit Haar measure, the average contribution of the syndrome s to the effective logical error rate is*

$$\mathbb{E}_{\text{Haar}}[\Delta_i(\overline{\mathcal{N}}_s)] = \frac{1}{2^{k+2}}. \quad (54)$$

Therefore, for an even-distance code, if all syndromes $s \in \mathcal{S}_{\Theta(1)}$ with non-vanishing conditional logical error rates satisfy the assumption of Lemma 1, the effective logical error rate decays exponentially with the number of logical qubits k :

Theorem 2. *Consider an $[[n, k, d]]$ stabilizer code with even distance d . Assume that for all $s \in \mathcal{S}_{\Theta(1)}$, the conditional noise channel \mathcal{N}_s is represented as $\mathcal{N}_s(\cdot) = \frac{1}{2} \cdot + \frac{1}{2} \overline{Q} \cdot \overline{Q}$, where logical Pauli- \overline{Q} operator that anti-commutes with the target logical operator \overline{P}_i is applied with probability $1/2$. Then, when the ideal logical quantum state $\overline{\rho}(\theta) = |\psi\rangle\langle\psi|$ is drawn from the k -qubit Haar*

measure, the average effective logical error rate $\epsilon_i^{\text{qSynd}}$ satisfies

$$\lim_{\eta \rightarrow 0} \frac{\mathbb{E}_{\text{Haar}}[\epsilon_i^{\text{qSynd}}]}{\epsilon_i} = \frac{1}{2^{k+1}}. \quad (55)$$

We leave the proofs of Lemma 1 and Theorem 2 to Appendix D3 and D4. Theorem 2 shows that, by performing syndrome-dependent logical measurements, the impact of errors on the estimator can be made exponentially small. This stands in stark contrast to classical protocols: when syndrome-dependent logical measurements are not allowed, the effective logical error rate is lower-bounded by a constant factor (Theorem 1). Meanwhile, once syndrome-conditioned logical measurements are allowed, the effective error rate can be exponentially small. Therefore, to fully exploit error-syndrome information at the logical estimation stage, syndrome-dependent logical measurements are necessary.

Let us discuss codes and noise models that satisfy the assumption of Theorem 2. First, consider an $[[n, 1, d]]$ code and choose the target logical operator \overline{P}_i to be a logical Z operator. In this case, $s \in \mathcal{S}_{\Theta(1)}$ corresponds to a syndrome caused by a weight- $d/2$ physical Pauli error, for which there exists another weight- $d/2$ physical Pauli error inducing a different logical action in terms of logical X or Y operators. If the conditional logical noise channel \mathcal{N}_s for such $s \in \mathcal{S}_{\Theta(1)}$ is a Pauli channel that applies the logical Pauli- X with probability $1/2$, then it satisfies the assumption of Theorem 2. Examples of such codes and noise models include the $[[d, 1, d]]$ repetition code under local bit-flip noise, the distance-2 rotated surface code $[[4, 1, 2]]$ under local depolarizing noise, and the $[[12, 1, 4]]$ code obtained from the $[[12, 2, 4]]$ carbon code [51] by promoting a Z -type logical operator to an additional stabilizer generator, under local depolarizing noise.

Now consider an $[[nk, k, d]]$ code composed of k blocks of such an $[[n, 1, d]]$ code, and choose \overline{P}_i to be a Z -type logical operator. In this case, $s \in \mathcal{S}_{\Theta(1)}$ corresponds to a syndrome caused by a weight- $d/2$ physical Pauli error within a single block. Therefore, the single-block discussion still applies, and the $[[nk, k, d]]$ code also satisfies the assumption of Theorem 2. Under such circumstances, we obtain an exponential decay in the effective logical error rate $\epsilon_i^{\text{qSynd}}$.

While Theorem 2 assumes a specific form of the conditional noise channels \mathcal{N}_s for $s \in \mathcal{S}_{\Theta(1)}$, we expect the exponential decay to be a generic feature of even-distance codes. We examine this by numerically evaluating $\epsilon_i^{\text{qSynd}}$ for other codes in Sec. VID. By contrast, for odd-distance codes we do not expect such an exponential decay. For odd-distance codes, the dominant contributions to $\epsilon_i^{\text{qSynd}}$ come not only from syndromes with non-vanishing conditional error rates, $s \in \mathcal{S}_{\Theta(1)}$, but also from syndromes with vanishing conditional error rates, $s \in \mathcal{S}_{\Theta(\eta)}$. Although the contribution from $s \in \mathcal{S}_{\Theta(1)}$ can be made exponentially small, the contribution from $s \in \mathcal{S}_{\Theta(\eta)}$ remains at the level of $\sum_{s \in \mathcal{S}_{\Theta(\eta)}} p_s \epsilon_{i,s}$. Therefore, as the

number of logical qubits k grows, we expect the effective logical error rate to approach $\sum_{s \in \mathcal{S}_{\Theta(\eta)}} p_s \epsilon_{i,s}$ and thus cannot become exponentially small. We numerically verify this intuition in Sec. VID.

We remark that the exponential suppression discussed above is an asymptotic statement in the low-error limit $\eta \rightarrow 0$, where the leading contribution to the (effective) logical error rate is governed by the ambiguous syndromes $s \in \mathcal{S}_{\Theta(1)}$. Meanwhile, at finite η , sub-leading syndromes that are higher order in η —which are neglected in the low-error limit—can eventually dominate once the leading-order contribution is reduced exponentially by the 2^{-k} factor. In particular, when $2^{-k} \lesssim \eta$, the leading-order estimate $2^{-k} \epsilon_i$ becomes as small as $O(\eta^{d/2+1})$, and sub-leading syndromes $s \notin \mathcal{S}_{\Theta(1)}$ can also affect $\epsilon_i^{\text{qSynd}}$. Since the contributions from such sub-leading syndromes may not be reduced exponentially, the exponential advantage may no longer be observable at finite η . Nevertheless, even in this regime, we still expect $\epsilon_i^{\text{qSynd}} = O(\eta^{d/2+1})$ when $2^{-k} \lesssim \eta$, which can be interpreted as an effective improvement of the code distance by 2 under quantum syndrome-aware protocols. This can be regarded as a different type of advantage enabled by quantum syndrome-aware protocols.

C. Optimal estimation protocol

In the previous subsection, we saw that the effective logical error rate $\epsilon_i^{\text{qSynd}}$ can be exponentially smaller than the logical error rate ϵ_i . Here, we investigate the optimal estimation protocol—namely, the optimal syndrome-dependent measurement basis—that achieves this exponential reduction, and discuss the underlying mechanism behind the exponential advantage. For this purpose, we consider the following simplified state:

$$\begin{aligned} & (1-p) |0\rangle\langle 0| \otimes \bar{\rho}(\boldsymbol{\theta}) + p |1\rangle\langle 1| \otimes \left(\frac{1}{2} \bar{\rho}(\boldsymbol{\theta}) + \frac{1}{2} \bar{Q} \bar{\rho}(\boldsymbol{\theta}) \bar{Q} \right) \\ &= (1-p) |0\rangle\langle 0| \otimes \bar{\rho}(\boldsymbol{\theta}) + p |1\rangle\langle 1| \otimes \bar{\rho}(\Lambda_{\bar{Q}} \boldsymbol{\theta}), \end{aligned} \quad (56)$$

where the Pauli operator \bar{Q} anti-commutes with the target logical observable \bar{P}_i . We analyze its quantum Fisher information and the corresponding optimal estimation protocol. Here, $\Lambda_{\bar{Q}}$ is a $(4^k - 1)$ -dimensional diagonal matrix whose (j, j) -th element is 1 if $[\bar{P}_j, \bar{Q}] = 0$ and 0 otherwise.

This state can be regarded as a coarse-grained version of the classical–quantum state arising in the setting of Theorem 2. We coarse-grain all syndromes $s \notin \mathcal{S}_{\Theta(1)}$ into a single label $s = 0$, with the corresponding syndrome-conditioned state approximated by $\bar{\rho}(\boldsymbol{\theta})$, by neglecting the vanishing conditional logical error $\epsilon_{i,s} \rightarrow 0$ as $\eta \rightarrow 0$. We then coarse-grain all syndromes $s \in \mathcal{S}_{\Theta(1)}$ into a single label $s = 1$, with the corresponding conditional state $\bar{\rho}(\Lambda_{\bar{Q}} \boldsymbol{\theta})$, which is affected by \bar{Q} with probability 1/2. Therefore, the state in Eq. (56) provides a good approxi-

mation of the low-error regime considered in Theorem 2.

When the observed syndrome is $s = 0$, we obtain the noiseless logical state $\bar{\rho}(\boldsymbol{\theta})$, and hence can extract full information, including the target expectation value $\theta_i = \text{tr}[\bar{\rho}(\boldsymbol{\theta}) \bar{P}_i]$ of the target logical observable \bar{P}_i . By contrast, when the observed syndrome is $s = 1$, we obtain the noisy logical state $\bar{\rho}(\Lambda_{\bar{Q}} \boldsymbol{\theta})$, from which we cannot extract information about θ_i because the target Pauli operator \bar{P}_i anti-commutes with \bar{Q} and thus $\bar{\rho}(\Lambda_{\bar{Q}} \boldsymbol{\theta})$ does not depend on θ_i . Nevertheless, we can still extract information about other parameters θ_j from $\bar{\rho}(\Lambda_{\bar{Q}} \boldsymbol{\theta})$, provided that the corresponding logical operator \bar{P}_j commutes with \bar{Q} . Such information about commuting Pauli components can then help reduce the uncertainty in estimating θ_i from the noiseless branch $\bar{\rho}(\boldsymbol{\theta})$. In other words, when the error syndrome $s = 1$ is observed, we can use $\bar{\rho}(\Lambda_{\bar{Q}} \boldsymbol{\theta})$ to estimate the commuting parameters θ_j with $[\bar{P}_j, \bar{Q}] = 0$ (which are unaffected by the \bar{Q} -error), and then treat them as effectively known when analyzing the $s = 0$ branch. This reduces the nuisance-parameter uncertainty and thereby improves the estimation of θ_i from the noiseless branch $\bar{\rho}(\boldsymbol{\theta})$.

To illustrate this mechanism, we consider the following auxiliary problem. Suppose we are given N copies of the noiseless logical state $\bar{\rho}(\boldsymbol{\theta})$ (corresponding to $s = 0$) and ask how knowledge of commuting parameters θ_j affects the estimation of θ_i . When we do not know all parameters $\boldsymbol{\theta} \in \mathbb{R}^{4^k - 1}$ —that is, when parameters θ_j with $j \neq i$ are treated as nuisance parameters [36]—the corresponding quantum Fisher information matrix is given by the inverse covariance matrix $C(\boldsymbol{\theta})^{-1} \in \mathbb{R}^{(4^k - 1) \times (4^k - 1)}$ defined in Eq. (44) (see Appendix B or Ref. [43] for the derivation). In this case, the optimal measurement basis is given by the target Pauli operator \bar{P}_i itself, and the optimal unbiased estimator θ_i^{est} is obtained by averaging the measurement outcomes. Indeed, $\mathbb{E}[\theta_i^{\text{est}}] = \text{tr}[\bar{\rho}(\boldsymbol{\theta}) \bar{P}_i] = \theta_i$, and its variance is $\text{Var}[\theta_i^{\text{est}}] = N^{-1}(\text{tr}[\bar{\rho}(\boldsymbol{\theta}) \bar{P}_i^2] - \text{tr}[\bar{\rho}(\boldsymbol{\theta}) \bar{P}_i]^2) = N^{-1}(1 - \theta_i^2) = N^{-1} C(\boldsymbol{\theta})_{ii}$, which attains the quantum Cramér–Rao bound in Eq. (8).

Now suppose that we have complete information about all parameters θ_j whose corresponding operators \bar{P}_j commute with \bar{Q} (which can, in principle, be estimated from the $s = 1$ branch $\bar{\rho}(\Lambda_{\bar{Q}} \boldsymbol{\theta})$). Let \mathcal{J}_+ denote the set of indices j such that \bar{P}_j commutes with \bar{Q} , and let \mathcal{J}_- denote those that anti-commute with \bar{Q} (note that $i \in \mathcal{J}_-$). Consider measuring $\bar{\rho}(\boldsymbol{\theta})$ with the operator

$$\bar{P}_i + \mathbf{n}_+^T \bar{\mathbf{P}}_+, \quad (57)$$

where $\mathbf{n}_+ \in \mathbb{R}^{2^{2k-1}-1}$ is a real vector and $\bar{\mathbf{P}}_+$ denotes the vector of logical Pauli operators with indices in \mathcal{J}_+ . The expectation value of this measurement is

$$\theta_i + \mathbf{n}_+^T \boldsymbol{\theta}_+, \quad (58)$$

where $\boldsymbol{\theta}_+$ denotes the vector of parameters θ_j with indices in \mathcal{J}_+ . Since the values of $\boldsymbol{\theta}_+$ are assumed to be

known, we can construct an unbiased estimator θ_i^{est} by measuring N copies of $\bar{\rho}(\boldsymbol{\theta})$ with $\bar{P}_i + \mathbf{n}_+^T \bar{\mathbf{P}}_+$ and subtracting $\mathbf{n}_+^T \boldsymbol{\theta}_+$ from the empirical average. The variance of this estimator is given by the variance of the operator $\bar{P}_i + \mathbf{n}_+^T \bar{\mathbf{P}}_+$, and we can minimize it over \mathbf{n}_+ . The minimum is achieved by choosing

$$\mathbf{n}_+^T = -\mathbf{e}_i^T C(\boldsymbol{\theta})_{-+} (C(\boldsymbol{\theta})_{++})^{-1}, \quad (59)$$

which yields the minimum variance

$$\text{Var}[\theta_i^{\text{est}}] = \frac{1}{N} \mathbf{e}_i^T ((C(\boldsymbol{\theta})^{-1})_{--})^{-1} \mathbf{e}_i. \quad (60)$$

Here, $+$ ($-$) denotes the block corresponding to indices in \mathcal{J}_+ (\mathcal{J}_-), and \mathbf{e}_i is now a 2^{2k-1} -dimensional unit vector. We also use the Schur complement identity $((C(\boldsymbol{\theta})^{-1})_{--})^{-1} = C(\boldsymbol{\theta})_{--} - C(\boldsymbol{\theta})_{-+} (C(\boldsymbol{\theta})_{++})^{-1} C(\boldsymbol{\theta})_{+-}$. For later convenience, we denote the corresponding optimal measurement operator as

$$\bar{P}_i - \bar{O}_i(\boldsymbol{\theta}) \quad (61)$$

with

$$\bar{O}_i(\boldsymbol{\theta}) = \mathbf{e}_i^T C(\boldsymbol{\theta})_{-+} (C(\boldsymbol{\theta})_{++})^{-1} \bar{\mathbf{P}}_+. \quad (62)$$

This estimator attains the quantum Cramér–Rao bound of the situation where the commuting parameters θ_j for $j \in \mathcal{J}_+$ are known and the anti-commuting parameters indexed by \mathcal{J}_- are unknown. In this case, the relevant quantum Fisher information matrix is $(C(\boldsymbol{\theta})^{-1})_{--} \in \mathbb{R}^{(4^k/2-1) \times (4^k/2-1)}$, so Eq. (60) achieves the quantum Cramér–Rao bound in Eq. (8). The key point is that the optimal measurement basis changes from \bar{P}_i to $\bar{P}_i - \bar{O}_i(\boldsymbol{\theta})$ once the commuting parameters θ_j for $j \in \mathcal{J}_+$ are known. This modification reduces the average uncertainty of the anti-commuting parameters. In particular, the Haar average of the inverse of the relevant quantum Fisher information matrix decays exponentially, as stated in the following proposition, whose proof is provided in Appendix D 2.

Proposition 3. *Let the ideal quantum state $\bar{\rho}(\boldsymbol{\theta}) = |\psi\rangle\langle\psi|$ be drawn from the k -qubit Haar measure. Then, the Haar average of the inverse of the quantum Fisher information matrix $(C(\boldsymbol{\theta})^{-1})_{--}$ in the setting where the parameters θ_j for $j \in \mathcal{J}_+$ are known and the anti-commuting parameters indexed by \mathcal{J}_- are unknown is given by*

$$\mathbb{E}_{\text{Haar}}[((C(\boldsymbol{\theta})^{-1})_{--})^{-1}] = \frac{1}{2^k} I. \quad (63)$$

Therefore, the estimator variance is exponentially reduced from $N^{-1}(1 - \theta_i^2) \sim N^{-1}$ to

$$\mathbb{E}_{\text{Haar}}[\text{Var}[\theta_i^{\text{est}}]] = \frac{1}{N} \mathbb{E}_{\text{Haar}}[\mathbf{e}_i^T ((C(\boldsymbol{\theta})^{-1})_{--})^{-1} \mathbf{e}_i] = \frac{1}{N} \frac{1}{2^k}. \quad (64)$$

We now return to the classical–quantum state in Eq. (56). As we will discuss in Appendix B, the inverse of the quantum Fisher information matrix of the classical–quantum state is

$$(J^{\text{Synd}})^{-1} = C(\boldsymbol{\theta}) + \frac{p}{1-p} \begin{pmatrix} 0 & 0 \\ 0 & ((C(\boldsymbol{\theta})^{-1})_{--})^{-1} \end{pmatrix}. \quad (65)$$

As discussed above, $(C(\boldsymbol{\theta})^{-1})_{--}$ is the quantum Fisher information matrix when the commuting parameters indexed by \mathcal{J}_+ are known while the anti-commuting parameters indexed by \mathcal{J}_- remain unknown. Thus, the increase in the variance induced by the noisy branch is governed by the residual uncertainty in the anti-commuting parameters given knowledge of the commuting ones. Since this uncertainty decays exponentially on average as in Proposition 3, we obtain an exponential advantage in quantum syndrome-aware protocols.

Finally, we describe an optimal quantum syndrome-aware estimation protocol for the simplified state in Eq. (56). As we will discuss in Appendix B, the optimal measurement basis defined through Eq. (9) for the target parameter θ_i is

$$|0\rangle\langle 0| \otimes \frac{1}{1-p} (\bar{P}_i - p \bar{O}_i(\boldsymbol{\theta})) + |1\rangle\langle 1| \otimes \bar{O}_i(\boldsymbol{\theta}). \quad (66)$$

Thus, an asymptotically optimal quantum syndrome-aware estimation protocol can be constructed as follows, which is based on an adaptive two-step strategy [37, 38].

1. Using the initial $N' = \lfloor \sqrt{N} \rfloor$ copies, construct a rough estimator $\boldsymbol{\theta}^{\text{init}}$ for all parameters.
2. For $t = N' + 1, \dots, N$, construct Δ_t from the remaining $N - N'$ copies as follows:
 - If the error syndrome $s = 0$ is obtained for the t -th copy, measure $\bar{\rho}(\boldsymbol{\theta})$ with the operator $\bar{P}_i - p \bar{O}_i(\boldsymbol{\theta}^{\text{init}})$ and obtain outcome o_t . Then set $\Delta_t = (o_t - \text{tr}[\bar{\rho}(\boldsymbol{\theta}^{\text{init}})(\bar{P}_i - p \bar{O}_i(\boldsymbol{\theta}^{\text{init}}))]) / (1 - p)$.
 - If the error syndrome $s = 1$ is obtained for the t -th copy, measure $\bar{\rho}(\Lambda_{\bar{Q}} \boldsymbol{\theta})$ with the operator $\bar{O}_i(\boldsymbol{\theta}^{\text{init}})$ and obtain outcome o_t . Then set $\Delta_t = o_t - \text{tr}[\bar{\rho}(\boldsymbol{\theta}^{\text{init}}) \bar{O}_i(\boldsymbol{\theta}^{\text{init}})]$.
3. Construct the estimator as $\theta_i^{\text{est}} = \theta_i^{\text{init}} + \frac{1}{N - N'} \sum_{t=N'+1}^N \Delta_t$.

Conditioned on the first-stage data (i.e., fixing $\boldsymbol{\theta}^{\text{init}}$), it is straightforward to verify that the expectation of θ_i^{est} over the remaining $N - N'$ copies equals θ_i . Hence, θ_i^{est} constructed above is an unbiased estimator of θ_i . Moreover, the variance of θ_i^{est} is obtained by averaging (over the first-stage data) the conditional variance given fixed $\boldsymbol{\theta}^{\text{init}}$. When $\boldsymbol{\theta}^{\text{init}} = \boldsymbol{\theta}$, the variance of Δ_t is $\mathbf{e}_i^T (J^{\text{Synd}})^{-1} \mathbf{e}_i$. Therefore, in the asymptotic limit $N \rightarrow \infty$ we typically have $\boldsymbol{\theta}^{\text{init}} \rightarrow \boldsymbol{\theta}$, resulting in $\text{Var}[\theta_i^{\text{est}}] \sim N^{-1} \mathbf{e}_i^T (J^{\text{Synd}})^{-1} \mathbf{e}_i$. Thus, the above estimator is asymptotically optimal and attains the quantum Cramér–Rao bound.

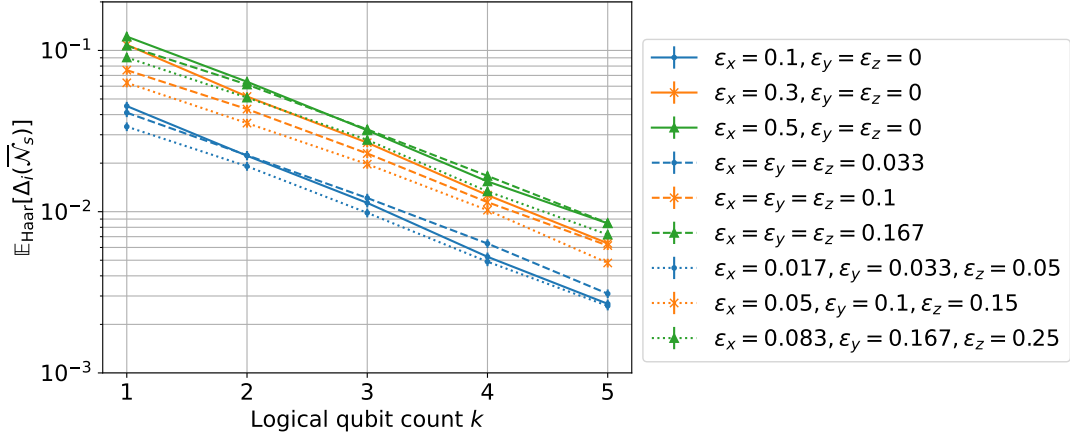


FIG. 5. Average contribution $\mathbb{E}_{\text{Haar}}[\Delta_i(\overline{\mathcal{N}}_s)]$ of ambiguous syndromes $s \in \mathcal{S}_{\Theta(1)}$ as a function of the number of logical qubits k . We assume the conditional noise channel $\overline{\mathcal{N}}_s = ((1 - \epsilon_x - \epsilon_y - \epsilon_z)\overline{\mathcal{I}} + \epsilon_x\overline{\mathcal{X}} + \epsilon_y\overline{\mathcal{Y}} + \epsilon_z\overline{\mathcal{Z}}) \otimes \overline{\mathcal{I}}^{\otimes(k-1)}$. The Haar average is estimated by sampling 1000 Haar-random states and averaging $\Delta_i(\overline{\mathcal{N}}_s)$ over the samples. Curves of the same color correspond to the same total logical error rate $\epsilon_x + \epsilon_y + \epsilon_z$, while curves with the same line style correspond to the same type of Pauli noise.

D. Numerical analysis

So far, we have shown that the effective logical error rate $\epsilon_i^{\text{qSynd}}$ for quantum syndrome-aware protocols can be exponentially smaller than the original logical error rate, provided that the assumption of Theorem 2 is satisfied. Here, we numerically investigate how broadly this exponential reduction persists beyond that assumption.

First, we study the average contribution $\Delta_i(\overline{\mathcal{N}}_s)$ of an ambiguous syndrome $s \in \mathcal{S}_{\Theta(1)}$, defined in Eq. (50). Lemma 1 shows that if the conditional noise channel takes the form $\overline{\mathcal{N}}_s(\cdot) = \frac{1}{2} \cdot + \frac{1}{2}\overline{Q} \cdot \overline{Q}$ for a Pauli operator \overline{Q} that anti-commutes with the target Pauli operator \overline{P}_i , then the contribution decays exponentially with k , namely $\mathbb{E}_{\text{Haar}}[\Delta_i(\overline{\mathcal{N}}_s)] = 2^{-(k+2)}$. We ask whether a similar exponential decay appears for more general conditional noise models. To this end, we consider an $[[nk, k, d]]$ stabilizer code composed of k blocks of an $[[n, 1, d]]$ stabilizer code. As discussed in Sec. VIB, a syndrome $s \in \mathcal{S}_{\Theta(1)}$ is characterized by an error localized to a single code block. Accordingly, when we take the target logical Pauli operator to be $\overline{P}_i = \overline{Z} \otimes \overline{I}^{\otimes(k-1)}$, the conditional logical noise channel for $s \in \mathcal{S}_{\Theta(1)}$ is represented as a local Pauli channel of the form

$$\overline{\mathcal{N}}_s = ((1 - \epsilon_x - \epsilon_y - \epsilon_z)\overline{\mathcal{I}} + \epsilon_x\overline{\mathcal{X}} + \epsilon_y\overline{\mathcal{Y}} + \epsilon_z\overline{\mathcal{Z}}) \otimes \overline{\mathcal{I}}^{\otimes(k-1)}. \quad (67)$$

Here, $\overline{\mathcal{I}}$ is the single-qubit logical identity channel, $\overline{\mathcal{X}}$, $\overline{\mathcal{Y}}$, and $\overline{\mathcal{Z}}$ are the single-qubit logical Pauli- X , Y , and Z channels, and ϵ_x , ϵ_y , and ϵ_z are the corresponding logical error probabilities. For this model, we evaluate $\mathbb{E}_{\text{Haar}}[\Delta_i(\overline{\mathcal{N}}_s)]$ as a function of the number of logical qubits k in Fig. 5. For all noise models we considered, we observe an exponential decay $\mathbb{E}_{\text{Haar}}[\Delta_i(\overline{\mathcal{N}}_s)] = O(2^{-k})$.

Next, we numerically evaluate the low-error-limit ratio

$\lim_{\eta \rightarrow 0} \mathbb{E}_{\text{Haar}}[\epsilon_i^{\text{qSynd}}]/\epsilon_i$ for several representative codes. We consider an $[[nk, k, d]]$ stabilizer code composed of k blocks of an $[[n, 1, d]]$ stabilizer code, and assume a local depolarizing noise model in which each physical qubit is independently affected by depolarizing noise with error rate η . We take the target logical Pauli operator to be $\overline{P}_i = \overline{Z} \otimes \overline{I}^{\otimes(k-1)}$. The results are shown in Fig. 6. For odd-distance codes, the ratio converges to a constant value. This aligns with the discussion in Sec. VIB, where syndromes $s \in \mathcal{S}_{\Theta(\eta)}$ with vanishing conditional logical error rate $\epsilon_{i,s} = O(\eta)$ also contribute at leading order to the (effective) logical error rates. Since such syndromes do not yield any benefit from syndrome-aware protocols, their leading-order contribution persists, preventing an exponential decay of the ratio. By contrast, for even-distance codes, we observe an exponential reduction in the effective logical error rate, with $\lim_{\eta \rightarrow 0} \mathbb{E}_{\text{Haar}}[\epsilon_i^{\text{qSynd}}]/\epsilon_i = O(2^{-k})$ for all codes we tested, including those that do not satisfy the assumption of Theorem 2.

These numerical results suggest that the exponential reduction of the effective logical error rate in the low-error regime may be a generic feature of even-distance codes. In this regime, ambiguous syndromes $s \in \mathcal{S}_{\Theta(1)}$ with non-vanishing conditional logical error rates govern the leading-order behavior of the (effective) logical error rate, and syndrome-dependent measurements allow one to extract useful information from such syndromes. This information can further help optimize the measurement basis on the nearly noiseless branch $s \notin \mathcal{S}_{\Theta(1)}$, as discussed in Sec. VIC. We leave a proof of this conjecture as an interesting direction for future work.

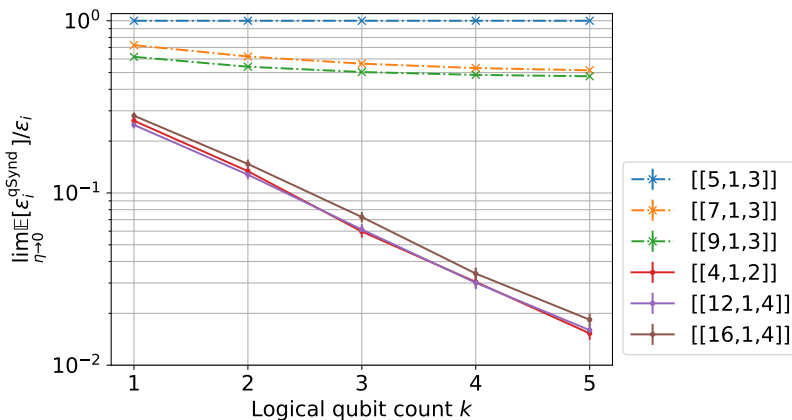


FIG. 6. Low-error-limit ratio $\lim_{\eta \rightarrow 0} \mathbb{E}_{\text{Haar}}[\epsilon_i^{\text{qSynd}}]/\epsilon_i$ as a function of the number of logical qubits k . The low-error-limit ratio $\lim_{\eta \rightarrow 0} \epsilon_i^{\text{qSynd}}/\epsilon_i$ is computed from Eqs. (52) and (53), and the Haar average is estimated by sampling 1000 Haar-random states. We consider the $[[5, 1, 3]]$ perfect code, $[[7, 1, 3]]$ Steane code, $[[9, 1, 3]]$ rotated surface code, $[[4, 1, 2]]$ rotated surface code, the $[[12, 1, 4]]$ code obtained from the $[[12, 2, 4]]$ carbon code [51] by promoting a Z -type logical operator to an additional stabilizer generator, and the $[[16, 1, 4]]$ rotated surface code. Solid (dash-dotted) lines correspond to even-distance (odd-distance) codes.

VII. DISCUSSION

In this work, we developed an information-theoretic framework to quantify the utility of error-syndrome information for noisy logical observable estimation. We introduced syndrome-agnostic, classical syndrome-aware, and quantum syndrome-aware estimation protocols and compared their achievable precision through Fisher information, summarized via an effective logical error rate. For classical syndrome-aware protocols—where the logical measurement basis is fixed and syndrome information is used only in classical post-processing—we proved a universal limitation showing that, on average, the effective logical error rate can improve by at most a factor of two. In contrast, when syndrome-conditioned logical measurement is permitted, we showed that this limitation can be violated: we identified settings in which the effective logical error rate becomes exponentially smaller with the number of logical qubits. We further clarified the mechanism behind this exponential advantage by analyzing the structure of the optimal syndrome-dependent measurement, and supported the generality of the phenomenon via numerical studies beyond the idealized assumptions used in our analytical constructions.

Our results establish a sharp separation between what can and cannot be gained from error-syndrome information in logical-layer estimation tasks. Our no-go theorem for classical syndrome-aware protocols shows that syndrome-dependent classical post-processing alone cannot remove the exponential sampling overhead inherent to logical-layer error mitigation, placing fundamental constraints on post-selection and related syndrome-conditioned classical strategies. At the same time, our exponential separations identify syndrome-conditioned quantum control—in particular, adapting the logical

measurement basis to the observed syndrome record—as the key ingredient that unlocks genuine exponential improvements. Conceptually, this highlights error syndromes as a form of side information whose value depends qualitatively on the allowed interface between decoding and logical control, and provides a principled criterion for when syndrome records should be actively exploited rather than discarded. Practically, our framework offers guidance for designing early fault-tolerant architectures and experimental protocols: if one seeks genuine gains in logical observable estimation, it is not sufficient to merely condition classical post-processing on syndrome data; one must instead enable syndrome-dependent quantum operations at the logical layer.

Future research could explore several promising directions. A particularly interesting direction is to prove an exponential reduction of the effective logical error rate for general even-distance codes. While our numerics suggest that such an exponential decay is generic, our analytical result establishes it only under the restricted assumptions of Theorem 2. Therefore, from a theoretical perspective, it would be important to generalize Theorem 2 to broader families of even-distance codes and noise models.

Another direction is to develop more practical quantum syndrome-aware estimation protocols. Although we proposed an asymptotically optimal protocol in Sec. VIC, it relies on characterizing the logical state in advance. Moreover, the required syndrome-dependent measurements are generally non-stabilizer measurements and thus may not be implementable fault-tolerantly without additional resources. It is therefore important, from a practical standpoint, to construct fault-tolerant quantum syndrome-aware protocols that use only stabilizer operations (or other native fault-tolerant primitives) and avoid extensive pre-characterization of the logical state.

We can further explore the utility of quantum syndrome-aware protocols for other tasks by considering alternative information measures. Here, we studied observable estimation through the quantum Fisher information of a classical–quantum state, where the classical register encodes the observed error syndrome and the quantum register is the corresponding syndrome-conditioned noisy logical state. Since syndrome-aware protocols can be modeled as operations on such classical–quantum states, the utility of syndrome information for other tasks may be analyzed by evaluating appropriate information measures on the same state. For example, advantages in quantum-state discrimination or hypothesis testing can be quantified via trace distance or relative entropy of the classical–quantum state. Such extensions would further broaden the applicability of our framework.

Finally, it will be crucial to develop early fault-tolerant algorithms that actively exploit syndrome information to further suppress the impact of errors. Since quantum syndrome-aware protocols can yield exponential improvements for logical observable estimation, it is natural to expect that adaptive modifications of logical operations conditioned on observed syndromes could also enhance algorithmic performance. Developing syndrome-adaptive variants of key primitives such as Hamiltonian simulation and phase estimation may therefore accelerate the practical deployment of early fault-tolerant devices.

ACKNOWLEDGEMENTS

The authors wish to thank discussion with Seok-Hyung Lee. K.T. is supported by the Program for Leading Graduate Schools (MERIT-WINGS) and JST BOOST Grant No. JPMJBS2418. H.K. is supported by the IITP (RS-2025-25464252) and the NRF (RS-2025-25464492, RS-2024-00442710) funded by the Ministry of Science and ICT (MSIT), Korea. L.J. is supported by the ARO(W911NF-23-1-0077), ARO MURI (W911NF-21-1-0325), AFOSR MURI (FA9550-21-1-0209, FA9550-23-1-0338), DARPA (HR0011-24-9-0359, HR0011-24-9-0361), NSF (ERC-1941583, OMA-2137642, OSI-2326767, CCF-2312755, OSI-2426975), and the Packard Foundation (2020-71479). N.Y. is supported by JST Grant Number JPMJPF2221, JST CREST Grant Number JPMJCR23I4, IBM Quantum, Google Quantum AI, JST ASPIRE Grant Number JPMJAP2316, JST ERATO Grant Number JPMJER2302, and Institute of AI and Beyond of the University of Tokyo.

Appendix A: Estimation protocol applied at the physical layer

In this section, we consider an estimation protocol performed directly on a noisy *physical* quantum state and show that it is equivalent (up to a unitary transformation) to the syndrome-aware estimation protocol, as illus-

trated in Fig. 1. Throughout this section, operators with $\bar{\cdot}$ act on the k -qubit logical Hilbert space, while operators without $\bar{\cdot}$ act on the n -qubit physical Hilbert space.

As in the main text, consider the task of preparing a k -qubit logical state

$$\bar{\rho}(\boldsymbol{\theta}) = \frac{1}{2^k} \left(\bar{I} + \sum_{i=1}^{4^k-1} \theta_i \bar{P}_i \right), \quad (\text{A1})$$

parameterized by an unnormalized generalized Bloch vector $\boldsymbol{\theta} = (\theta_1, \dots, \theta_{4^k-1})$ [39]. Our goal is to estimate the expectation value of a logical Pauli operator \bar{P}_i , i.e., the parameter $\theta_i = \text{tr}[\bar{\rho}(\boldsymbol{\theta})\bar{P}_i]$. Here, $\{\bar{P}_i\}_{i=0}^{4^k-1}$ denotes the set of k -qubit Pauli operators, with $\bar{P}_0 = \bar{I}$.

When the device is subject to noise, we encode $\bar{\rho}(\boldsymbol{\theta})$ into an n -qubit physical state using an $[[n, k, d]]$ stabilizer code. Let $\{g_a\}_{a=1}^m$ be a set of stabilizer generators with $m = n - k$, and let $\{P_i\}_{i=1}^{4^k-1}$ be a choice of physical representatives of the nontrivial logical Pauli operators. We describe encoding by an isometry channel $\mathcal{U}_E(\cdot) = U_E \cdot U_E^\dagger$, which can be implemented as

$$\mathcal{U}_E(\cdot) = U_E'(|0^m\rangle\langle 0^m| \otimes \cdot) U_E'^{\dagger}, \quad (\text{A2})$$

where the unitary U_E' satisfies

$$\begin{aligned} U_E' Z_a U_E'^{\dagger} &= g_a & (1 \leq a \leq m), \\ U_E' (I_m \otimes \bar{P}_i) U_E'^{\dagger} &= P_i & (1 \leq i \leq 4^k - 1). \end{aligned} \quad (\text{A3})$$

Here, I_m is the identity operator on the m -qubit ancilla system and Z_a is the Pauli- Z operator acting on the a -th ancilla qubit.

The encoded physical state $\rho(\boldsymbol{\theta}) = \mathcal{U}_E(\bar{\rho}(\boldsymbol{\theta}))$ can be written as

$$\begin{aligned} \rho(\boldsymbol{\theta}) &= U_E' \left(\prod_{a=1}^m \frac{1}{2} (I + Z_a) \right) \frac{1}{2^k} \left(I + \sum_{i=1}^{4^k-1} \theta_i I_m \otimes \bar{P}_i \right) U_E'^{\dagger} \\ &= \Pi_0 \frac{1}{2^k} \left(I + \sum_{i=1}^{4^k-1} \theta_i P_i \right), \end{aligned} \quad (\text{A4})$$

where, for each syndrome $s \in \{0, 1\}^m$, we define the projector

$$\Pi_s = \prod_{a=1}^m \frac{1}{2} (I + (-1)^{s_a} g_a). \quad (\text{A5})$$

Next, consider a physical Pauli channel $\mathcal{E}_Q(\cdot) = Q \cdot Q^\dagger$. Then,

$$\mathcal{E}_Q(\rho(\boldsymbol{\theta})) = \Pi_s \frac{1}{2^k} \left(I + \sum_{i=1}^{4^k-1} (-1)^{\langle P_i, Q \rangle} \theta_i P_i \right), \quad (\text{A6})$$

where we define $\langle P, Q \rangle = 0$ if P and Q commute and $\langle P, Q \rangle = 1$ if they anticommute. The syndrome $s \in$

$\{0, 1\}^m$ associated with Q is determined by $s_a = \langle g_a, Q \rangle$. Therefore, after physical Pauli noise channel \mathcal{N} acts on $\rho(\boldsymbol{\theta})$, the state can be decomposed into syndrome sectors as

$$\mathcal{N}(\rho(\boldsymbol{\theta})) = \sum_{s \in \{0,1\}^m} p_s \Pi_s \frac{1}{2^k} \left(I + \sum_{i=1}^{4^k-1} \lambda_{i,s} \theta_i P_i \right), \quad (\text{A7})$$

where $p_s \geq 0$ with $\sum_s p_s = 1$ is the probability of obtaining syndrome s , and $\lambda_{i,s} \in [-1, 1]$ describes the Pauli eigenvalue associated with P_i .

We now perform syndrome measurement followed by a Pauli recovery. Upon observing syndrome s , we apply a Pauli operator R_s such that $\langle g_a, R_s \rangle = s_a$ for all a . The resulting corrected state through the recovery channel \mathcal{R} is

$$\begin{aligned} & \mathcal{R} \circ \mathcal{N}(\rho(\boldsymbol{\theta})) \\ &= \Pi_0 \frac{1}{2^k} \left(I + \sum_{i=1}^{4^k-1} \left(\sum_{s \in \{0,1\}^m} p_s (-1)^{\langle P_i, R_s \rangle} \lambda_{i,s} \right) \theta_i P_i \right). \end{aligned} \quad (\text{A8})$$

Defining the induced logical noise channel

$$\bar{\mathcal{N}} = \mathcal{U}_E^\dagger \circ \mathcal{R} \circ \mathcal{N} \circ \mathcal{U}_E, \quad (\text{A9})$$

we obtain

$$\bar{\mathcal{N}}(\bar{\rho}(\boldsymbol{\theta})) = \frac{1}{2^k} \left(\bar{I} + \sum_{i=1}^{4^k-1} (1 - 2\epsilon_i) \theta_i \bar{P}_i \right), \quad (\text{A10})$$

where

$$\epsilon_i = \frac{1}{2} \left(1 - \sum_{s \in \{0,1\}^m} p_s (-1)^{\langle P_i, R_s \rangle} \lambda_{i,s} \right). \quad (\text{A11})$$

On the other hand, applying $(U_E')^\dagger$ to the noisy physical state $\mathcal{N}(\rho(\boldsymbol{\theta}))$ yields a unitarily equivalent state of the form

$$\mathcal{N}(\rho(\boldsymbol{\theta})) \cong \sum_{s \in \{0,1\}^m} p_s |s\rangle\langle s| \otimes \frac{1}{2^k} \left(\bar{I} + \sum_{i=1}^{4^k-1} \lambda_{i,s} \theta_i \bar{P}_i \right), \quad (\text{A12})$$

where \cong means unitary equivalence. Moreover, by applying an s -conditioned logical Pauli correction \bar{R}_s satisfying $\langle P_i, R_s \rangle = \langle \bar{P}_i, \bar{R}_s \rangle$ for all i , we obtain

$$\mathcal{N}(\rho(\boldsymbol{\theta})) \cong \sum_{s \in \{0,1\}^m} p_s |s\rangle\langle s| \otimes \bar{\mathcal{N}}_s(\bar{\rho}(\boldsymbol{\theta})), \quad (\text{A13})$$

where the s -conditioned noise channel is given as

$$\bar{\mathcal{N}}_s(\bar{\rho}(\boldsymbol{\theta})) = \frac{1}{2^k} \left(\bar{I} + \sum_{i=1}^{4^k-1} (1 - 2\epsilon_{i,s}) \theta_i \bar{P}_i \right) \quad (\text{A14})$$

with

$$\epsilon_{i,s} = \frac{1}{2} \left(1 - (-1)^{\langle P_i, R_s \rangle} \lambda_{i,s} \right). \quad (\text{A15})$$

Therefore, the noisy physical state $\mathcal{N}(\rho(\boldsymbol{\theta}))$ is unitarily equivalent to the classical-quantum state $\sum_s p_s |s\rangle\langle s| \otimes \bar{\mathcal{N}}_s(\bar{\rho}(\boldsymbol{\theta}))$ used to model syndrome-aware estimation in the main text.

Since the quantum Fisher information is invariant under unitary transformations, any estimation protocol performed directly on the noisy physical state $\mathcal{N}(\rho(\boldsymbol{\theta}))$ can be mapped to a quantum syndrome-aware estimation protocol acting on $\sum_s p_s |s\rangle\langle s| \otimes \bar{\mathcal{N}}_s(\bar{\rho}(\boldsymbol{\theta}))$ with the same achievable precision. In particular, protocols that perform estimation directly at the physical layer—including physical-level error-mitigation schemes such as those studied in Ref. [61]—can be interpreted within our framework as quantum syndrome-aware estimation protocols that retain and exploit the syndrome record. Therefore, the information difference between the physical-state setting and the usual syndrome-agnostic logical-state setting is solely characterized by whether the syndrome information is kept or discarded.

Appendix B: Quantum Fisher information of multi-qubit quantum state

In this section, based on Ref. [43], we review the quantum Fisher information of noiseless and noisy multi-qubit quantum states. Moreover, we analyze the quantum Fisher information of the classical-quantum state in Eq. (56).

1. Analysis of noiseless multi-qubit quantum state

First, we review the quantum Fisher information of a k -qubit quantum state parameterized as

$$\bar{\rho}(\boldsymbol{\theta}) = \frac{1}{2^k} \left(\bar{I} + \sum_{i=1}^{4^k-1} \theta_i \bar{P}_i \right). \quad (\text{B1})$$

Here, the parameters $\boldsymbol{\theta} = (\theta_1, \dots, \theta_{4^k-1})$ form an unnormalized Bloch vector [39], which represents the expectation value of the Pauli operator \bar{P}_i as $\theta_i = \text{tr}[\bar{\rho}(\boldsymbol{\theta}) \bar{P}_i]$. By defining the covariance matrix $C(\boldsymbol{\theta})$ of this state as

$$\begin{aligned} C(\boldsymbol{\theta})_{ij} &= \text{tr} \left[\bar{\rho}(\boldsymbol{\theta}) \frac{1}{2} \{ \bar{P}_i - \theta_i \bar{I}, \bar{P}_j - \theta_j \bar{I} \} \right] \\ &= \text{tr} \left[\bar{\rho}(\boldsymbol{\theta}) \frac{1}{2} \{ \bar{P}_i, \bar{P}_j \} \right] - \text{tr}[\bar{\rho}(\boldsymbol{\theta}) \bar{P}_i] \text{tr}[\bar{\rho}(\boldsymbol{\theta}) \bar{P}_j], \end{aligned} \quad (\text{B2})$$

the SLD operator \bar{L}_i of this state, defined as in Eq. (5), can be represented as

$$\bar{L}_i = \sum_j (C(\boldsymbol{\theta})^{-1})_{ij} (\bar{P}_j - \theta_j \bar{I}). \quad (\text{B3})$$

This is because the SLD operator \bar{L}_i satisfies

$$\begin{aligned} \text{tr}[\bar{\rho}(\boldsymbol{\theta})\frac{1}{2}\{\bar{L}_i, \bar{P}_j - \theta_j\bar{I}\}] &= \text{tr}\left[\frac{1}{2}\{\bar{\rho}(\boldsymbol{\theta}), \bar{L}_i\}(\bar{P}_j - \theta_j\bar{I})\right] \\ &= \text{tr}[\partial_{\theta_i}\bar{\rho}(\boldsymbol{\theta})(\bar{P}_j - \theta_j\bar{I})] \\ &= \text{tr}[2^{-k}\bar{P}_i(\bar{P}_j - \theta_j\bar{I})] \\ &= \delta_{ij}. \end{aligned} \quad (\text{B4})$$

Therefore, the quantum Fisher information matrix J , defined in Eq. (6), is given as

$$J = C(\boldsymbol{\theta})^{-1}C(\boldsymbol{\theta})C(\boldsymbol{\theta})^{-1} = C(\boldsymbol{\theta})^{-1}, \quad (\text{B5})$$

and the quantum Fisher information for the parameter $\text{tr}[\bar{\rho}(\boldsymbol{\theta})\bar{P}] = \theta_i$, defined in Eq. (7), is given as

$$J_{\theta_i} = \frac{1}{(J^{-1})_{ii}} = \frac{1}{C(\boldsymbol{\theta})_{ii}} = \frac{1}{1 - \theta_i^2}. \quad (\text{B6})$$

Assume that our goal is to estimate the parameter $\theta_i = \text{tr}[\bar{\rho}(\boldsymbol{\theta})\bar{P}_i]$ given N copies of $\bar{\rho}(\boldsymbol{\theta})$, in the situation where all the parameters in $\boldsymbol{\theta}$ are unknown. In this case, the optimal measurement operator, given by Eq. (9), is

$$\sum_j (J^{-1})_{ij}\bar{L}_j = \bar{P}_i - \theta_i\bar{I}. \quad (\text{B7})$$

Therefore, the optimal measurement basis is given by the target Pauli operator \bar{P}_i itself, and the optimal unbiased estimator θ_i^{est} is obtained by averaging the measurement outcomes. Indeed, $\mathbb{E}[\theta_i^{\text{est}}] = \text{tr}[\bar{\rho}(\boldsymbol{\theta})\bar{P}_i] = \theta_i$, and its variance is $\text{Var}[\theta_i^{\text{est}}] = N^{-1}(\text{tr}[\bar{\rho}(\boldsymbol{\theta})\bar{P}_i^2] - \text{tr}[\bar{\rho}(\boldsymbol{\theta})\bar{P}_i]^2) = N^{-1}(1 - \theta_i^2)$, which attains the quantum Cramér–Rao bound in Eq. (8).

2. Analysis of noisy multi-qubit quantum state

Next, we consider the case where the quantum state $\bar{\rho}(\boldsymbol{\theta})$ is affected by a noise channel $\bar{\mathcal{N}}$, resulting in a noisy quantum state

$$\bar{\mathcal{N}}(\bar{\rho}(\boldsymbol{\theta})) = \frac{1}{2^k} \left(\bar{I} + \sum_{i=1}^{4^k-1} ((A\boldsymbol{\theta})_i + c_i)\bar{P}_i \right). \quad (\text{B8})$$

Here, $A \in \mathbb{R}^{(4^k-1) \times (4^k-1)}$ is a Pauli transfer matrix defined as $A_{ij} = 2^{-k}\text{tr}[\bar{P}_i\bar{\mathcal{N}}(\bar{P}_j)]$, and $c_i = 2^{-k}\text{tr}[\bar{P}_i\bar{\mathcal{N}}(\bar{I})]$. By defining the modified parameter $\boldsymbol{\theta}' = A\boldsymbol{\theta} + \mathbf{c}$, the noisy state can be represented as $\bar{\mathcal{N}}(\bar{\rho}(\boldsymbol{\theta})) = \bar{\rho}(\boldsymbol{\theta}')$. For $\bar{\rho}(\boldsymbol{\theta}')$, the SLD operators and quantum Fisher information matrix in terms of the parameters $\boldsymbol{\theta}'$ can be represented as

$$\bar{L}'_i = \sum_j (C(\boldsymbol{\theta}')^{-1})_{ij}(\bar{P}_j - \theta'_j\bar{I}), \quad (\text{B9})$$

$$J' = C(\boldsymbol{\theta}')^{-1}. \quad (\text{B10})$$

Meanwhile, the SLD operators and quantum Fisher information matrices under the two parameterizations $\boldsymbol{\theta}$ and $\boldsymbol{\theta}'$ are related as

$$\bar{L}_i = \sum_j \frac{\partial\theta'_j}{\partial\theta_i}\bar{L}'_j = \sum_j (A^T)_{ij}\bar{L}'_j, \quad (\text{B11})$$

$$J_{ij} = \sum_{kl} \frac{\partial\theta'_k}{\partial\theta_i}J'_{kl}\frac{\partial\theta'_l}{\partial\theta_j} = \sum_{kl} (A^T)_{ik}J'_{kl}A_{lj}. \quad (\text{B12})$$

Therefore, the SLD operators and the quantum Fisher information matrix of the noisy state $\bar{\mathcal{N}}(\bar{\rho}(\boldsymbol{\theta}))$ in terms of the parameters $\boldsymbol{\theta}$ are

$$\bar{L}_i = \sum_{jk} (A^T)_{ij}(C(A\boldsymbol{\theta} + \mathbf{c})^{-1})_{jk}(\bar{P}_k - \theta'_k\bar{I}), \quad (\text{B13})$$

$$J = A^T C(A\boldsymbol{\theta} + \mathbf{c})^{-1} A, \quad (\text{B14})$$

and the quantum Fisher information for the parameter $\theta_i = \text{tr}[\bar{\rho}(\boldsymbol{\theta})\bar{P}]$ is given as

$$J_{\theta_i} = \frac{1}{(A^{-1}C(A\boldsymbol{\theta} + \mathbf{c})(A^T)^{-1})_{ii}}. \quad (\text{B15})$$

Consider the task of estimating the parameter $\theta_i = \text{tr}[\bar{\rho}(\boldsymbol{\theta})\bar{P}_i]$ given N copies of the noisy state $\bar{\mathcal{N}}(\bar{\rho}(\boldsymbol{\theta}))$. In this case, we have

$$\sum_j (J^{-1})_{ij}\bar{L}_j = (A^{-1})_{ij}(\bar{P}_j - \theta'_j\bar{I}) = (\bar{\mathcal{N}}^{-1})^\dagger(\bar{P}_i) + a\bar{I} \quad (\text{B16})$$

for some $a \in \mathbb{R}$. Therefore, the optimal measurement basis is given by $(\bar{\mathcal{N}}^{-1})^\dagger(\bar{P}_i)$, and the optimal unbiased estimator θ_i^{est} is obtained by averaging the measurement outcomes. Indeed, $\mathbb{E}[\theta_i^{\text{est}}] = \text{tr}[\bar{\mathcal{N}}(\bar{\rho}(\boldsymbol{\theta}))(\bar{\mathcal{N}}^{-1})^\dagger(\bar{P}_i)] = \theta_i$, and its variance is $\text{Var}[\theta_i^{\text{est}}] = N^{-1}(A^{-1}C(A\boldsymbol{\theta} + \mathbf{c})(A^T)^{-1})_{ii}$, which attains the quantum Cramér–Rao bound in Eq. (8).

In the main text, we especially consider the case where the noise channel $\bar{\mathcal{N}}$ is a Pauli channel, so $A = \Lambda$ becomes a diagonal matrix and $\mathbf{c} = 0$. By representing $\Lambda = \text{diag}(1 - 2\epsilon_1, \dots, 1 - 2\epsilon_{4^k-1})$, the optimal measurement basis is represented as $(\bar{\mathcal{N}}^{-1})^\dagger(\bar{P}_i) = (1 - 2\epsilon_i)^{-1}\bar{P}_i$. Therefore, the optimal estimation protocol boils down to measuring the noisy state $\bar{\mathcal{N}}(\bar{\rho}(\boldsymbol{\theta}))$ with the original Pauli operator \bar{P}_i , and then rescaling the measurement outcome by a factor of $(1 - 2\epsilon_i)^{-1}$.

3. Analysis of the classical–quantum state in Eq. (56)

Finally, we analyze the quantum Fisher information of the classical–quantum state in Eq. (56):

$$\begin{aligned} &(1-p)|0\rangle\langle 0| \otimes \bar{\rho}(\boldsymbol{\theta}) + p|1\rangle\langle 1| \otimes \left(\frac{1}{2}\bar{\rho}(\boldsymbol{\theta}) + \frac{1}{2}\bar{Q}\bar{\rho}(\boldsymbol{\theta})\bar{Q} \right) \\ &= (1-p)|0\rangle\langle 0| \otimes \bar{\rho}(\boldsymbol{\theta}) + p|1\rangle\langle 1| \otimes \bar{\rho}(\Lambda_{\bar{Q}}\boldsymbol{\theta}). \end{aligned} \quad (\text{B17})$$

Here, \bar{Q} is a Pauli operator and $\Lambda_{\bar{Q}}$ is a $(4^k - 1)$ -dimensional diagonal matrix whose (j, j) -th element is 1 if $[\bar{P}_j, \bar{Q}] = 0$ and 0 otherwise. From Eq. (45), the quantum Fisher information matrix of this state is represented as

$$J^{\text{Synd}} = (1 - p)C(\boldsymbol{\theta})^{-1} + p\Lambda_{\bar{Q}}C(\Lambda_{\bar{Q}}\boldsymbol{\theta})^{-1}\Lambda_{\bar{Q}}. \quad (\text{B18})$$

Let \mathcal{J}_+ denote the set of indices j such that \bar{P}_j commutes with \bar{Q} , and let \mathcal{J}_- denote those that anti-commute with \bar{Q} . Then, the inverse of the quantum Fisher information matrix can be written as

$$(J^{\text{Synd}})^{-1} = C(\boldsymbol{\theta}) + \frac{p}{1-p} \begin{pmatrix} 0 & 0 \\ 0 & ((C(\boldsymbol{\theta})^{-1})_{--})^{-1} \end{pmatrix}. \quad (\text{B19})$$

Here, $+$ ($-$) denotes the block corresponding to indices in \mathcal{J}_+ (\mathcal{J}_-), and we use the Woodbury matrix identity $(A + UCV)^{-1} = A^{-1} - A^{-1}U(C^{-1} + VA^{-1}U)^{-1}VA^{-1}$ together with the Schur complement identity $((C(\boldsymbol{\theta})^{-1})_{--})^{-1} = C(\boldsymbol{\theta})_{--} - C(\boldsymbol{\theta})_{-+}(C(\boldsymbol{\theta})_{++})^{-1}C(\boldsymbol{\theta})_{+-}$. Meanwhile, from Eq. (12) and Eq. (B3), the SLD operator \bar{L}_j of this state is given by

$$\begin{aligned} & |0\rangle\langle 0| \otimes e_j^T C(\boldsymbol{\theta})^{-1}(\bar{\mathbf{P}} - \boldsymbol{\theta}\bar{I}) \\ & + |1\rangle\langle 1| \otimes e_j^T (C(\boldsymbol{\theta})_{++})^{-1}(\bar{\mathbf{P}}_+ - \boldsymbol{\theta}_+\bar{I}) \end{aligned} \quad (\text{B20})$$

for $j \in \mathcal{J}_+$, and by

$$|0\rangle\langle 0| \otimes e_j^T C(\boldsymbol{\theta})^{-1}(\bar{\mathbf{P}} - \boldsymbol{\theta}\bar{I}) \quad (\text{B21})$$

for $j \in \mathcal{J}_-$. Here, $\bar{\mathbf{P}}$ denotes the vector of all nontrivial Pauli operators \bar{P}_j , and $\bar{\mathbf{P}}_+$ and $\boldsymbol{\theta}_+$ denote the subvectors restricted to indices $j \in \mathcal{J}_+$. Therefore, the optimal measurement basis defined through Eq. (9) for estimating the target parameter θ_i with $i \in \mathcal{J}_-$ is

$$|0\rangle\langle 0| \otimes \frac{1}{1-p}(\bar{P}_i - p\bar{O}_i(\boldsymbol{\theta})) + |1\rangle\langle 1| \otimes \bar{O}_i(\boldsymbol{\theta}), \quad (\text{B22})$$

where

$$\bar{O}_i(\boldsymbol{\theta}) = e_i^T C(\boldsymbol{\theta})_{-+}(C(\boldsymbol{\theta})_{++})^{-1}\bar{\mathbf{P}}_+. \quad (\text{B23})$$

Note that we use $((C(\boldsymbol{\theta})^{-1})_{--})^{-1}(C(\boldsymbol{\theta})^{-1})_{-+} = -C(\boldsymbol{\theta})_{-+}(C(\boldsymbol{\theta})_{++})^{-1}$ from the Schur complement.

Appendix C: Proof of the results for classical syndrome-aware protocols

In this section, we provide detailed proofs of the results for classical syndrome-aware protocols discussed in Sec. V.

1. Proof of Theorem 1

Proof. From the definition, the effective logical error rate satisfies

$$\begin{aligned} \epsilon_i^{\text{cSynd}} &= f_{\theta_i}^{-1} \left(\sum_{s \in \mathcal{S}} p_s f_{\theta_i}(\epsilon_{i,s}) \right) \\ &\leq \sum_{s \in \mathcal{S}} p_s f_{\theta_i}^{-1}(f_{\theta_i}(\epsilon_{i,s})) \\ &= \sum_{s \in \mathcal{S}} p_s \epsilon_{i,s} \\ &= \epsilon_i. \end{aligned} \quad (\text{C1})$$

Here, $f_{\theta_i}^{-1}$ is the inverse function of

$$f_{\theta_i}(\epsilon) = \frac{(1 - 2\epsilon)^2}{1 - (1 - 2\epsilon)^2 \theta_i^2} \quad (\text{C2})$$

defined in Eq. (23) on the domain $0 \leq \epsilon \leq 1/2$. The first equality follows from the definition of the effective logical error rate in Eq. (28). The next inequality follows from Jensen's inequality (since $f_{\theta_i}^{-1}$ is convex). The last equality follows from Eq. (18). Moreover, from the convexity of $f_{\theta_i}^{-1}$, we have

$$\begin{aligned} \epsilon_{i,s} &= f_{\theta_i}^{-1}(f_{\theta_i}(\epsilon_{i,s})) \\ &\leq \frac{f_{\theta_i}^{-1}(f_{\theta_i}(0)) - f_{\theta_i}^{-1}(f_{\theta_i}(1/2))}{f_{\theta_i}(0) - f_{\theta_i}(1/2)} (f_{\theta_i}(\epsilon_{i,s}) - f_{\theta_i}(1/2)) \\ &\quad + f_{\theta_i}^{-1}(f_{\theta_i}(1/2)) \\ &= -\frac{1 - \theta_i^2}{2} f_{\theta_i}(\epsilon_{i,s}) + \frac{1}{2}. \end{aligned} \quad (\text{C3})$$

Multiplying by p_s and summing over $s \in \mathcal{S}$, we obtain

$$\begin{aligned} \epsilon_i &\leq -\frac{1 - \theta_i^2}{2} f_{\theta_i}(\epsilon_i^{\text{cSynd}}) + \frac{1}{2} \\ &= \epsilon_i^{\text{cSynd}} \frac{2 - 2\epsilon_i^{\text{cSynd}}}{1 - \theta_i^2(1 - 2\epsilon_i^{\text{cSynd}})^2}. \end{aligned} \quad (\text{C4})$$

Meanwhile, we have

$$\frac{2 - 2\epsilon_i^{\text{cSynd}}}{1 - \theta_i^2(1 - 2\epsilon_i^{\text{cSynd}})^2} \leq \frac{2}{1 - \theta_i^2}, \quad (\text{C5})$$

since the left-hand side is maximized when $\epsilon_i^{\text{cSynd}} = 0$. By combining Eqs. (C1), (C4), (C5), we obtain

$$\frac{1 - \theta_i^2}{2} \epsilon_i \leq \epsilon_i^{\text{cSynd}} \leq \epsilon_i. \quad (\text{C6})$$

The Haar-average result follows from the fact that

$$\mathbb{E}_{\text{Haar}}[\theta_i^2] = \mathbb{E}_{\text{Haar}}[\text{tr}[|\psi\rangle\langle\psi| \bar{P}_i^2]] = \frac{1}{2^k + 1}. \quad (\text{C7})$$

See Ref. [62] for details. \square

2. Proof of Corollary 1

Proof. From Theorem 1, we have

$$\frac{1 - \theta_i^2}{2} \epsilon_i \leq \epsilon_i^{\text{cSynd}} \leq \epsilon_i. \quad (\text{C8})$$

This implies that if $\epsilon_i = \Theta(\eta^l)$, then $\epsilon_i^{\text{cSynd}} = \Theta(\eta^l)$, assuming $\theta_i \neq \pm 1$.

Moreover, the code threshold for the logical error rate ϵ_i (respectively, the effective logical error rate $\epsilon_i^{\text{cSynd}}$) is defined as the maximal physical error rate such that, if η is below this value, $\epsilon_i \rightarrow 0$ (respectively, $\epsilon_i^{\text{cSynd}} \rightarrow 0$) as the code distance d increases. From Eq. (C8), $\epsilon_i \rightarrow 0$ implies $\epsilon_i^{\text{cSynd}} \rightarrow 0$, and $\epsilon_i^{\text{cSynd}} \rightarrow 0$ implies $\epsilon_i \rightarrow 0$. Therefore, the threshold defined in terms of the effective logical error rate $\epsilon_i^{\text{cSynd}}$ is identical to that defined in terms of the logical error rate ϵ_i under the maximum-likelihood decoder. \square

3. Proof of Corollary 2

Proof. Since $N^{\text{cSynd}} \leq N^{\text{L}}$ is obvious from Eq. (27), we prove the other inequality. From Eq. (C3), we have

$$f_{\theta_i}(\epsilon_{i,s}) \leq \frac{1 - 2\epsilon_{i,s}}{1 - \theta_i^2}. \quad (\text{C9})$$

Multiplying by p_s and summing over $s \in \mathcal{S}$, we obtain

$$F_{\theta_i}^{\text{Synd}} \leq \frac{1 - 2\epsilon_i}{1 - \theta_i^2} = \frac{1}{1 - \theta_i^2} \sqrt{\frac{f_{\theta_i}(\epsilon_i)}{1 + \theta_i^2 f_{\theta_i}(\epsilon_i)}}. \quad (\text{C10})$$

Taking the inverse of the above inequality, we obtain

$$(1 - \theta_i^2) \sqrt{(F_{\theta_i}^{\text{L}})^{-1} + \theta_i^2} \leq (F_{\theta_i}^{\text{Synd}})^{-1}. \quad (\text{C11})$$

Dividing both sides by σ_{target}^2 yields the claimed inequality.

The Haar-average results follow from the fact that

$$\begin{aligned} \mathbb{E}_{\text{Haar}}[N^{\text{cSynd}}] &= \frac{\mathbb{E}_{\text{Haar}}[(F_{\theta_i}^{\text{Synd}})^{-1}]}{\sigma_{\text{target}}^2} \\ &\geq \frac{1 - \mathbb{E}_{\text{Haar}}[\theta_i^2]}{\sigma_{\text{target}}^2 (1 - 2\epsilon_i)} \\ &= \frac{1}{\sigma_{\text{target}}^2 (1 - 2\epsilon_i)} \frac{2^k}{2^k + 1} \\ &\sim \frac{1}{\sigma_{\text{target}}^2 (1 - 2\epsilon_i)}, \end{aligned} \quad (\text{C12})$$

and

$$\begin{aligned} \mathbb{E}_{\text{Haar}}[N^{\text{L}}] &= \frac{\mathbb{E}_{\text{Haar}}[(F_{\theta_i}^{\text{L}})^{-1}]}{\sigma_{\text{target}}^2} \\ &= \frac{1}{\sigma_{\text{target}}^2} \left(\frac{1}{(1 - 2\epsilon_i)^2} - \mathbb{E}_{\text{Haar}}[\theta_i^2] \right) \\ &= \frac{1}{\sigma_{\text{target}}^2} \left(\frac{1}{(1 - 2\epsilon_i)^2} - \frac{1}{2^k + 1} \right) \\ &\sim \frac{1}{\sigma_{\text{target}}^2} \frac{1}{(1 - 2\epsilon_i)^2}. \end{aligned} \quad (\text{C13})$$

Here, we use Eqs. (22), (C7), and (C10). \square

4. Proof of Proposition 1

Proof. From Eq. (37), we have

$$\lim_{\eta \rightarrow 0} \frac{\epsilon_i^{\text{cSynd}}}{\epsilon_i} = \lim_{\eta \rightarrow 0} \frac{\sum_{s \in \mathcal{S}_{\Theta(1)}} p_s (f_{\theta_i}(\epsilon_{i,s}) - f_{\theta_i}(0))}{\sum_{s \in \mathcal{S}_{\Theta(1)}} p_s f_{\theta_i}^{(1)} \epsilon_{i,s}}. \quad (\text{C14})$$

Here, we expand the function $f_{\theta_i}(\epsilon)$ around $\epsilon = 0$ as $f_{\theta_i}(\epsilon) = f_{\theta_i}(0) + f_{\theta_i}^{(1)} \epsilon + O(\epsilon^2)$, where $f_{\theta_i}^{(1)} = -4(1 - \theta_i^2)^{-2}$. From the convexity of the function $f_{\theta_i}(\epsilon)$, we have

$$\frac{1 - \theta_i^2}{2} \leq \frac{f_{\theta_i}(\epsilon_{i,s}) - f_{\theta_i}(0)}{f_{\theta_i}^{(1)} \epsilon_{i,s}} < 1 \quad (\text{C15})$$

for $s \in \mathcal{S}_{\Theta(1)}$, where $0 < \epsilon_{i,s} \leq 1/2$. The equality holds if and only if $\epsilon_{i,s} = 1/2$. Combining Eqs. (C14) and (C15), we obtain the claimed inequality in Proposition 1. \square

5. Proof of Proposition 2

Proof. From Eq. (39), we have

$$\begin{aligned} \lim_{\eta \rightarrow 0} \frac{\epsilon_i^{\text{cSynd}}}{\epsilon_i} &= \lim_{\eta \rightarrow 0} \frac{\sum_{s \in \mathcal{S}_{\Theta(\eta)}} p_s f_{\theta_i}^{(1)} \epsilon_{i,s} + \sum_{s \in \mathcal{S}_{\Theta(1)}} p_s (f_{\theta_i}(\epsilon_{i,s}) - f_{\theta_i}(0))}{\sum_{s \in \mathcal{S}_{\Theta(\eta)}} p_s f_{\theta_i}^{(1)} \epsilon_{i,s} + \sum_{s \in \mathcal{S}_{\Theta(1)}} p_s f_{\theta_i}^{(1)} \epsilon_{i,s}}. \end{aligned} \quad (\text{C16})$$

For $s \in \mathcal{S}_{\Theta(1)}$ (where $0 < \epsilon_{i,s} \leq 1/2$), we have

$$\frac{1 - \theta_i^2}{2} \leq \frac{f_{\theta_i}(\epsilon_{i,s}) - f_{\theta_i}(0)}{f_{\theta_i}^{(1)} \epsilon_{i,s}} < 1. \quad (\text{C17})$$

Therefore, the limit ratio satisfies $\lim_{\eta \rightarrow 0} \epsilon_i^{\text{cSynd}} / \epsilon_i < 1$ if and only if $\mathcal{S}_{\Theta(1)} \neq \emptyset$. \square

Appendix D: Proof of the results for quantum syndrome-aware protocols

In this section, we provide detailed proofs of the results for quantum syndrome-aware protocols discussed in

Sec. VI. Before presenting the proofs, we first introduce a useful lemma about the covariance matrix $C(\boldsymbol{\theta})$ for a pure state. We then prove Proposition 3, Lemma 1, and Theorem 2 in this order.

Before going into details, we note that the ideal logical state $\bar{\rho}(\boldsymbol{\theta})$ should be of full rank for the covariance matrix $C(\boldsymbol{\theta})$ to have an inverse. Therefore, strictly speaking, whenever an inverse matrix appears, we take the ideal state to be a Haar-random state affected by a small depolarizing noise, $\bar{\rho}((1-\delta)\boldsymbol{\theta}) = (1-\delta)|\psi\rangle\langle\psi| + \delta\frac{\bar{I}}{2^k}$, and then take $\delta \rightarrow 0$ after the calculation. Accordingly, when writing $\mathbb{E}_{\text{Haar}}[f(\boldsymbol{\theta})]$ for some function f in which matrix inversion appears, we mean that we first take the Haar average of $f((1-\delta)\boldsymbol{\theta})$ over Haar-random states $|\psi\rangle$, and then take the limit $\delta \rightarrow 0$. Nevertheless, in most cases where $f(\boldsymbol{\theta})$ does not involve matrix inversion, we can simply set $\delta = 0$ and take the average. Therefore, we regard the ideal logical state as $\bar{\rho}((1-\delta)\boldsymbol{\theta})$ only when an explicit calculation involving matrix inversion is required.

1. Properties of the covariance matrix of a pure state

For a k -qubit quantum state

$$\bar{\rho}(\boldsymbol{\theta}) = \frac{1}{2^k} \left(\bar{I} + \sum_{i=1}^{4^k-1} \theta_i \bar{P}_i \right), \quad (\text{D1})$$

we have defined its covariance matrix as

$$C(\boldsymbol{\theta})_{ij} = \text{tr} \left[\bar{\rho}(\boldsymbol{\theta}) \frac{1}{2} \{ \bar{P}_i, \bar{P}_j \} \right] - \text{tr}[\bar{\rho}(\boldsymbol{\theta}) \bar{P}_i] \text{tr}[\bar{\rho}(\boldsymbol{\theta}) \bar{P}_j]. \quad (\text{D2})$$

In particular, when $\bar{\rho}(\boldsymbol{\theta}) = |\psi\rangle\langle\psi|$ is a pure state, we obtain the following lemma.

Lemma 2. *Let $\bar{\rho}(\boldsymbol{\theta}) = |\psi\rangle\langle\psi|$ be a pure state. Then, the corresponding $(4^k-1) \times (4^k-1)$ covariance matrix $C(\boldsymbol{\theta})$ has the following properties:*

- $C(\boldsymbol{\theta})\boldsymbol{\theta} = \mathbf{0}$.
- $C(\boldsymbol{\theta})$ has eigenvalues 0 and 2^{k-1} with multiplicities $(2^k-1)^2$ and $2(2^k-1)$, respectively.

Proof. For $\boldsymbol{o} \in \mathbb{R}^{4^k-1}$, define an observable $\bar{O} = \sum_i o_i \bar{P}_i$. Let $\{|\psi_i\rangle\}_{i=1}^{2^k}$ denote an orthonormal basis of the k -qubit Hilbert space with $|\psi_1\rangle = |\psi\rangle$, and write the matrix representation of \bar{O} in this basis as

$$\begin{pmatrix} a & \mathbf{h}^\dagger \\ \mathbf{h} & B \end{pmatrix} \quad (\text{D3})$$

with $a \in \mathbb{C}$, $\mathbf{h} \in \mathbb{C}^{2^k-1}$, and $B \in \mathbb{C}^{(2^k-1) \times (2^k-1)}$ satisfying $a + \text{tr}[B] = 0$. Note that the first row and column correspond to $|\psi_1\rangle = |\psi\rangle$. Then,

$$\boldsymbol{o}^\text{T} C(\boldsymbol{\theta}) \boldsymbol{o} = \langle\psi|\bar{O}^2|\psi\rangle - \langle\psi|\bar{O}|\psi\rangle^2 = \|\mathbf{h}\|^2. \quad (\text{D4})$$

This implies that if the operator $\bar{O} = \sum_i o_i \bar{P}_i$ is of the form

$$\begin{pmatrix} a & \mathbf{0}^\dagger \\ \mathbf{0} & B \end{pmatrix}, \quad (\text{D5})$$

then the corresponding vector \boldsymbol{o} belongs to the kernel of $C(\boldsymbol{\theta})$. Since $\sum_i \theta_i \bar{P}_i = 2^k |\psi\rangle\langle\psi| - \bar{I}$ is of this form, we have $C(\boldsymbol{\theta})\boldsymbol{\theta} = \mathbf{0}$. Moreover, since a Hermitian matrix $B \in \mathbb{C}^{(2^k-1) \times (2^k-1)}$ has $(2^k-1)^2$ real degrees of freedom, the dimension of the kernel of $C(\boldsymbol{\theta})$ is $(2^k-1)^2$.

Meanwhile, the image of $C(\boldsymbol{\theta})$ is spanned by vectors \boldsymbol{o} whose corresponding operators $\bar{O} = \sum_i o_i \bar{P}_i$ are of the form

$$\begin{pmatrix} \mathbf{0} & \mathbf{h}^\dagger \\ \mathbf{h} & \mathbf{0} \end{pmatrix}. \quad (\text{D6})$$

Let us choose an orthonormal basis $\{\boldsymbol{o}_i\}_{i=1}^{2(2^k-1)}$ of the support such that $\bar{O}_i = \sum_j (\boldsymbol{o}_i)_j \bar{P}_j$ is given by

$$\begin{aligned} & 2^{(k-1)/2} (|\psi\rangle\langle\psi_{(i+3)/2}| + |\psi_{(i+3)/2}\rangle\langle\psi|) \quad (i: \text{odd}), \\ & 2^{(k-1)/2} i (|\psi\rangle\langle\psi_{i/2+1}| - |\psi_{i/2+1}\rangle\langle\psi|) \quad (i: \text{even}). \end{aligned} \quad (\text{D7})$$

We can check the orthonormality of this basis as $\boldsymbol{o}_i^\text{T} \boldsymbol{o}_j = 2^{-k} \text{tr}[\bar{O}_i \bar{O}_j] = \delta_{ij}$. Moreover,

$$\boldsymbol{o}_i^\text{T} C(\boldsymbol{\theta}) \boldsymbol{o}_j = \frac{1}{2} \langle\psi|\{\bar{O}_i, \bar{O}_j\}|\psi\rangle = 2^{k-1} \delta_{ij}. \quad (\text{D8})$$

This means that all the nonzero eigenvalues of $C(\boldsymbol{\theta})$ are 2^{k-1} . Therefore, $C(\boldsymbol{\theta})$ has eigenvalues 0 and 2^{k-1} with multiplicities $(2^k-1)^2$ and $2(2^k-1)$, respectively. \square

2. Proof of Proposition 3

Proof. Let an orthonormal matrix V denote the Pauli transfer matrix of a unitary operator \bar{U} , i.e., $V_{ij} = 2^{-k} \text{tr}[\bar{P}_i \bar{U} \bar{P}_j \bar{U}^\dagger]$. As in the main text, we denote by $\Lambda_{\bar{Q}}$ the (4^k-1) -dimensional diagonal matrix whose (j, j) -th entry is 1 if $[\bar{P}_j, \bar{Q}] = 0$ and 0 otherwise. If V commutes with $\Lambda_{\bar{Q}}$, i.e., $V_{-+} = V_{+-} = 0$, we have

$$\begin{aligned} & \mathbb{E}_{\text{Haar}}[(C(\boldsymbol{\theta})^{-1})_{--}]^{-1} \\ &= \mathbb{E}_{\text{Haar}}[(C(V\boldsymbol{\theta})^{-1})_{--}]^{-1} \\ &= V_{--} \mathbb{E}_{\text{Haar}}[(C(\boldsymbol{\theta})^{-1})_{--}]^{-1} (V_{--})^\text{T}. \end{aligned} \quad (\text{D9})$$

Here, we use the fact that $\mathbb{E}_{\text{Haar}}[f(\boldsymbol{\theta})] = \mathbb{E}_{\text{Haar}}[f(V\boldsymbol{\theta})]$ and $C(V\boldsymbol{\theta}) = VC(\boldsymbol{\theta})V^\text{T}$. Let \bar{U} be a Pauli operator that anti-commutes with \bar{P}_a and commutes with \bar{P}_b . In this case, V is a diagonal matrix with $V_{aa} = -1$ and $V_{bb} = 1$, so we have

$$\begin{aligned} & (\mathbb{E}_{\text{Haar}}[(C(\boldsymbol{\theta})^{-1})_{--}]^{-1})_{ab} \\ &= -(\mathbb{E}_{\text{Haar}}[(C(\boldsymbol{\theta})^{-1})_{--}]^{-1})_{ab}. \end{aligned} \quad (\text{D10})$$

This implies that the off-diagonal element ($a \neq b$) is 0, so $\mathbb{E}_{\text{Haar}}[(C(\boldsymbol{\theta})^{-1})_{--}]^{-1}$ is diagonal.

Moreover, there always exists a Clifford unitary operator \bar{U} which leaves \bar{Q} unchanged (up to an overall phase of ± 1) and swaps two Pauli operators \bar{P}_a and \bar{P}_b that anti-commute with \bar{Q} . Since such a Clifford unitary \bar{U} maps Pauli operators commuting (anti-commuting) with \bar{Q} to Pauli operators commuting (anti-commuting) with \bar{Q} , we have $V_{-+} = V_{+-} = 0$. Moreover, when V is applied to a vector, the a -th and b -th components are swapped. Therefore, by applying this orthonormal matrix V to Eq. (D9), its (a, a) -th and (b, b) -th diagonal elements must be identical. Thus, we obtain

$$\begin{aligned} & \mathbb{E}_{\text{Haar}}[\text{tr}[(C(\boldsymbol{\theta})^{-1})_{--}]^{-1}] \\ &= \mathbb{E}_{\text{Haar}}[\text{tr}[(C(\boldsymbol{\theta})^{-1})_{--}]^{-1}] \frac{I}{2^{2k-1}}. \end{aligned} \quad (\text{D11})$$

Let us calculate the trace of the matrix. By considering the Schur complement, we obtain

$$\begin{aligned} & \text{tr}[(C(\boldsymbol{\theta})^{-1})_{--}]^{-1} \\ &= \text{tr}[C(\boldsymbol{\theta})_{--}] - \text{tr}[C(\boldsymbol{\theta})_{-+}(C(\boldsymbol{\theta})_{++})^{-1}C(\boldsymbol{\theta})_{+-}]. \end{aligned} \quad (\text{D12})$$

Meanwhile, by considering $((C(\boldsymbol{\theta}))^2)_{++}$, we have

$$(C(\boldsymbol{\theta})_{++})^2 + C(\boldsymbol{\theta})_{+-}C(\boldsymbol{\theta})_{-+} = ((C(\boldsymbol{\theta}))^2)_{++}. \quad (\text{D13})$$

By multiplying $(C(\boldsymbol{\theta})_{++})^{-1}$ and taking the trace, we obtain

$$\begin{aligned} & \text{tr}[C(\boldsymbol{\theta})_{-+}(C(\boldsymbol{\theta})_{++})^{-1}C(\boldsymbol{\theta})_{+-}] \\ &= -\text{tr}[C(\boldsymbol{\theta})_{++}] + \text{tr}[(C(\boldsymbol{\theta})_{++})^{-1}((C(\boldsymbol{\theta}))^2)_{++}], \end{aligned} \quad (\text{D14})$$

which leads to

$$\begin{aligned} & \text{tr}[(C(\boldsymbol{\theta})^{-1})_{--}]^{-1} \\ &= \text{tr}[C(\boldsymbol{\theta})] - \text{tr}[(C(\boldsymbol{\theta})_{++})^{-1}((C(\boldsymbol{\theta}))^2)_{++}]. \end{aligned} \quad (\text{D15})$$

For an accurate calculation of this value, we need to replace $\boldsymbol{\theta}$ with $(1 - \delta)\boldsymbol{\theta}$ and take $\delta \rightarrow 0$. Under this treatment, we can regard the inverse matrix as a pseudo-inverse matrix by considering an eigenvalue decomposition of the matrices $C((1 - \delta)\boldsymbol{\theta})_{++}$ and $((C((1 - \delta)\boldsymbol{\theta}))^2)_{++}$ and taking $\delta \rightarrow 0$. From Lemma 2, we recall that the covariance matrix $C(\boldsymbol{\theta})$ can be represented as

$$C(\boldsymbol{\theta}) = 2^{k-1}\Pi_{\text{Im}}, \quad (\text{D16})$$

where Π_{Im} represents the projector onto the image of $C(\boldsymbol{\theta})$, whose dimension is $2(2^k - 1)$. Therefore, we have

$$\begin{aligned} & \lim_{\delta \rightarrow 0} \text{tr}[(C((1 - \delta)\boldsymbol{\theta})_{++})^{-1}((C((1 - \delta)\boldsymbol{\theta}))^2)_{++}] \\ &= 2^{k-1} \text{tr}[(\Pi_{\text{Im}})_{++}]^{\text{pinv}} (\Pi_{\text{Im}})_{++}] \\ &= 2^{k-1} (\text{dim}(\text{Im}(C(\boldsymbol{\theta}))) - \text{dim}(\text{Im}(C(\boldsymbol{\theta})) \cap \text{Im}(\Pi_-))). \end{aligned} \quad (\text{D17})$$

Here, $((\Pi_{\text{Im}})_{++})^{\text{pinv}}$ is the pseudo-inverse matrix of $(\Pi_{\text{Im}})_{++}$, $\Pi_- = I - \Lambda_{\bar{Q}}$ is a projector to the subspace spanned by anti-commuting parameters indexed by

$j \in \mathcal{J}_-$, $\text{Im}(\cdot)$ represents the image of \cdot , and $\text{dim}(\cdot)$ represents the dimension of a vector space \cdot . The second equality follows from the fact that $\text{tr}[(\Pi_{\text{Im}})_{++}]^{\text{pinv}} (\Pi_{\text{Im}})_{++}]$ equals the dimension of the image of the linear map $\boldsymbol{o} \in \text{Im}(C(\boldsymbol{\theta})) \mapsto \Lambda_{\bar{Q}}\boldsymbol{o}$, together with the rank-nullity theorem. Therefore, we obtain

$$\begin{aligned} & \text{tr}[(C(\boldsymbol{\theta})^{-1})_{--}]^{-1} \\ &= 2^{k-1} \text{dim}(\text{Im}(C(\boldsymbol{\theta})) \cap \text{Im}(\Pi_-)). \end{aligned} \quad (\text{D18})$$

Now, we analyze the dimension of $\text{Im}(C(\boldsymbol{\theta})) \cap \text{Im}(\Pi_-)$. From the proof of Lemma 2, we note that when $\boldsymbol{o} \in \text{Im}(C(\boldsymbol{\theta}))$, the corresponding operator $\sum_i o_i \bar{P}_i$ is of the form

$$\sum_i o_i \bar{P}_i = |\psi\rangle\langle w| + |w\rangle\langle\psi|, \quad (\text{D19})$$

where $|w\rangle \in \mathbb{C}^{2^k}$ with $|w\rangle \perp |\psi\rangle$. Moreover, when $\boldsymbol{o} \in \text{Im}(\Pi_-)$, the operator $\sum_i o_i \bar{P}_i$ should anti-commute with \bar{Q} . Denote $|\psi\rangle = |\psi_{+1}\rangle + |\psi_{-1}\rangle$ and $|w\rangle = |w_{+1}\rangle + |w_{-1}\rangle$, where $|\psi_{\pm 1}\rangle$ and $|w_{\pm 1}\rangle$ belong to the ± 1 eigenspace of \bar{Q} . Then, we have $\bar{Q}(|\psi\rangle\langle w| + |w\rangle\langle\psi|) + (|\psi\rangle\langle w| + |w\rangle\langle\psi|)\bar{Q} = 0$ if and only if

$$\begin{aligned} & |\psi_{+1}\rangle\langle w_{+1}| + |w_{+1}\rangle\langle\psi_{+1}| = 0, \\ & |\psi_{-1}\rangle\langle w_{-1}| + |w_{-1}\rangle\langle\psi_{-1}| = 0. \end{aligned} \quad (\text{D20})$$

By multiplying $|\psi_{\pm 1}\rangle$ from the right, we obtain

$$|w_{+1}\rangle = ia_{+1} |\psi_{+1}\rangle, \quad |w_{-1}\rangle = ia_{-1} |\psi_{-1}\rangle, \quad (\text{D21})$$

where $a_{\pm 1} \in \mathbb{R}$. Moreover, since $|w\rangle \perp |\psi\rangle$, we have

$$a_{+1} \langle\psi_{+1}|\psi_{+1}\rangle + a_{-1} \langle\psi_{-1}|\psi_{-1}\rangle = 0. \quad (\text{D22})$$

Therefore, $\boldsymbol{o} \in \text{Im}(C(\boldsymbol{\theta})) \cap \text{Im}(\Pi_-)$ if and only if there exist $a_{\pm 1} \in \mathbb{R}$ satisfying

$$\begin{aligned} & \sum_i o_i \bar{P}_i = i \left(-|\psi\rangle (a_{+1} \langle\psi_{+1}| + a_{-1} \langle\psi_{-1}|) \right. \\ & \quad \left. + (a_{+1} |\psi_{+1}\rangle + a_{-1} |\psi_{-1}\rangle) \langle\psi| \right), \\ & a_{+1} \langle\psi_{+1}|\psi_{+1}\rangle + a_{-1} \langle\psi_{-1}|\psi_{-1}\rangle = 0. \end{aligned} \quad (\text{D23})$$

This means that $\boldsymbol{o} \in \text{Im}(C(\boldsymbol{\theta})) \cap \text{Im}(\Pi_-)$ is characterized by a single real parameter, so

$$\text{dim}(\text{Im}(C(\boldsymbol{\theta})) \cap \text{Im}(\Pi_-)) = 1. \quad (\text{D24})$$

From Eqs. (D11), (D18), and (D24), we obtain

$$\mathbb{E}_{\text{Haar}}[\text{tr}[(C(\boldsymbol{\theta})^{-1})_{--}]^{-1}] = \frac{1}{2^k} I. \quad (\text{D25})$$

□

3. Proof of Lemma 1

Proof. For the Pauli noise channel $\bar{\mathcal{N}}_s(\cdot) = \frac{1}{2} \cdot + \frac{1}{2} \bar{Q} \cdot \bar{Q}$, we analyze

$$\Delta_i(\bar{\mathcal{N}}_s) = \frac{\mathbf{e}_i^T (C(\boldsymbol{\theta}) - C(\boldsymbol{\theta}) \Lambda_{\bar{Q}} C(\Lambda_{\bar{Q}} \boldsymbol{\theta})^{-1} \Lambda_{\bar{Q}} C(\boldsymbol{\theta})) \mathbf{e}_i}{4}. \quad (\text{D26})$$

Here, $\Lambda_{\bar{Q}}$ is a $(4^k - 1)$ -dimensional diagonal matrix whose (j, j) -th element is 1 if $[\bar{P}_j, \bar{Q}] = 0$ and 0 otherwise. Let us write the covariance matrix as

$$C(\boldsymbol{\theta}) = \begin{pmatrix} C(\boldsymbol{\theta})_{++} & C(\boldsymbol{\theta})_{+-} \\ C(\boldsymbol{\theta})_{-+} & C(\boldsymbol{\theta})_{--} \end{pmatrix}. \quad (\text{D27})$$

For the covariance matrix $C(\Lambda_{\bar{Q}} \boldsymbol{\theta})$, we have

$$C(\Lambda_{\bar{Q}} \boldsymbol{\theta}) = \begin{pmatrix} C(\boldsymbol{\theta})_{++} & 0 \\ 0 & C(\Lambda_{\bar{Q}} \boldsymbol{\theta})_{--} \end{pmatrix}. \quad (\text{D28})$$

Here, we use the fact that when \bar{P}_i commutes and \bar{P}_j anticommutes with \bar{Q} , the product $\bar{P}_i \bar{P}_j$ anticommutes with \bar{Q} , so the off-diagonal blocks of $C(\Lambda_{\bar{Q}} \boldsymbol{\theta})$ become 0. Moreover, by definition,

$$\Lambda_{\bar{Q}} = \begin{pmatrix} I & 0 \\ 0 & 0 \end{pmatrix}. \quad (\text{D29})$$

Therefore,

$$\begin{aligned} & C(\boldsymbol{\theta}) - C(\boldsymbol{\theta}) \Lambda_{\bar{Q}} C(\Lambda_{\bar{Q}} \boldsymbol{\theta})^{-1} \Lambda_{\bar{Q}} C(\boldsymbol{\theta}) \\ &= \begin{pmatrix} 0 & 0 \\ 0 & C(\boldsymbol{\theta})_{--} - C(\boldsymbol{\theta})_{-+} C(\boldsymbol{\theta})_{++}^{-1} C(\boldsymbol{\theta})_{+-} \end{pmatrix}, \end{aligned} \quad (\text{D30})$$

resulting in

$$\begin{aligned} \Delta_i(\bar{\mathcal{N}}_s) &= \frac{\mathbf{e}_i^T (C(\boldsymbol{\theta})_{--} - C(\boldsymbol{\theta})_{-+} C(\boldsymbol{\theta})_{++}^{-1} C(\boldsymbol{\theta})_{+-}) \mathbf{e}_i}{4} \\ &= \frac{\mathbf{e}_i^T ((C(\boldsymbol{\theta})^{-1})_{--})^{-1} \mathbf{e}_i}{4} \end{aligned} \quad (\text{D31})$$

from the Schur complement.

Taking the Haar average and combining with Proposition 3, we obtain

$$\mathbb{E}_{\text{Haar}}[\Delta_i(\bar{\mathcal{N}}_s)] = \frac{1}{2^{k+2}}. \quad (\text{D32})$$

□

4. Proof of Theorem 2

Proof. From Eq. (52), we have

$$\lim_{\eta \rightarrow 0} \frac{\mathbb{E}_{\text{Haar}}[\epsilon_i^{\text{qSynd}}]}{\epsilon_i} = \lim_{\eta \rightarrow 0} \frac{\sum_{s \in \mathcal{S}_{\Theta(1)}} p_s \mathbb{E}_{\text{Haar}}[\Delta_i(\bar{\mathcal{N}}_s)]}{\sum_{s \in \mathcal{S}_{\Theta(1)}} p_s \epsilon_{i,s}}. \quad (\text{D33})$$

Under the assumption of Theorem 2, for all $s \in \mathcal{S}_{\Theta(1)}$ we have

$$\epsilon_{i,s} = \frac{1}{2}, \quad (\text{D34})$$

and by Lemma 1,

$$\mathbb{E}_{\text{Haar}}[\Delta_i(\bar{\mathcal{N}}_s)] = \frac{1}{2^{k+2}}. \quad (\text{D35})$$

Therefore, we obtain

$$\lim_{\eta \rightarrow 0} \frac{\mathbb{E}_{\text{Haar}}[\epsilon_i^{\text{qSynd}}]}{\epsilon_i} = \frac{1}{2^{k+1}}. \quad (\text{D36})$$

□

-
- [1] P. W. Shor, Scheme for reducing decoherence in quantum computer memory, *Phys. Rev. A* **52**, R2493 (1995).
- [2] E. Knill, R. Laflamme, and W. Zurek, Threshold accuracy for quantum computation, [arXiv:quant-ph/9610011](https://arxiv.org/abs/quant-ph/9610011) (1996).
- [3] D. Aharonov and M. Ben-Or, Fault-tolerant quantum computation with constant error, in *Proc. 29th Annu. ACM Symp. Theory Comput.* (ACM, El Paso, Texas, USA, 1997) pp. 176–188.
- [4] D. A. Lidar and T. A. Brun, *Quantum error correction* (Cambridge university press, Cambridge, UK, 2013).
- [5] N. Ofek, A. Petrenko, R. Heeres, P. Reinhold, Z. Leghtas, B. Vlastakis, Y. Liu, L. Frunzio, S. Girvin, L. Jiang, *et al.*, Extending the lifetime of a quantum bit with error correction in superconducting circuits, *Nature* **536**, 441 (2016).
- [6] S. Krinner, N. Lacroix, A. Remm, A. Di Paolo, E. Genois, C. Leroux, C. Hellings, S. Lazar, F. Swiadek, J. Herrmann, *et al.*, Realizing repeated quantum error correction in a distance-three surface code, *Nature* **605**, 669 (2022).
- [7] Google Quantum AI, Suppressing quantum errors by scaling a surface code logical qubit, *Nature* **614**, 676 (2023).
- [8] V. Sivak, A. Eickbusch, B. Royer, S. Singh, I. Tsioutsios, S. Ganjam, A. Miano, B. Brock, A. Ding, L. Frunzio, *et al.*, Real-time quantum error correction beyond break-even, *Nature* **616**, 50 (2023).
- [9] D. Bluvstein, S. J. Evered, A. A. Geim, S. H. Li, H. Zhou, T. Manovitz, S. Ebadi, M. Cain, M. Kalinowski,

- D. Hangleiter, *et al.*, Logical quantum processor based on reconfigurable atom arrays, *Nature* **626**, 58 (2024).
- [10] Google Quantum AI and Collaborators, Quantum error correction below the surface code threshold, *Nature* **638**, 920 (2024).
- [11] K. Temme, S. Bravyi, and J. M. Gambetta, Error mitigation for short-depth quantum circuits, *Phys. Rev. Lett.* **119**, 180509 (2017).
- [12] S. Endo, Z. Cai, S. C. Benjamin, and X. Yuan, Hybrid quantum-classical algorithms and quantum error mitigation, *J. Phys. Soc. Japan* **90**, 032001 (2021).
- [13] Z. Cai, R. Babbush, S. C. Benjamin, S. Endo, W. J. Huggins, Y. Li, J. R. McClean, and T. E. O'Brien, Quantum error mitigation, *Rev. Mod. Phys.* **95**, 045005 (2023).
- [14] Y. Kim, A. Eddins, S. Anand, K. X. Wei, E. Van Den Berg, S. Rosenblatt, H. Nayfeh, Y. Wu, M. Zaletel, K. Temme, *et al.*, Evidence for the utility of quantum computing before fault tolerance, *Nature* **618**, 500 (2023).
- [15] C. Piveteau, D. Sutter, S. Bravyi, J. M. Gambetta, and K. Temme, Error mitigation for universal gates on encoded qubits, *Phys. Rev. Lett.* **127**, 200505 (2021).
- [16] M. Lostaglio and A. Ciani, Error mitigation and quantum-assisted simulation in the error corrected regime, *Phys. Rev. Lett.* **127**, 200506 (2021).
- [17] Y. Suzuki, S. Endo, K. Fujii, and Y. Tokunaga, Quantum error mitigation as a universal error reduction technique: Applications from the nisq to the fault-tolerant quantum computing eras, *PRX Quantum* **3**, 010345 (2022).
- [18] K. Tsubouchi, Y. Mitsuhashi, K. Sharma, and N. Yoshioka, Symmetric clifford twirling for cost-optimal quantum error mitigation in early ftqc regime, *npj Quantum Information* **11**, 104 (2025).
- [19] H. Bombín, M. Pant, S. Roberts, and K. I. Seetharam, Fault-tolerant postselection for low-overhead magic state preparation, *PRX Quantum* **5**, 010302 (2024).
- [20] N. Meister, C. A. Pattison, and J. Preskill, Efficient soft-output decoders for the surface code, [arXiv:2405.07433](https://arxiv.org/abs/2405.07433) (2024).
- [21] S. C. Smith, B. J. Brown, and S. D. Bartlett, Mitigating errors in logical qubits, *Commun. Phys.* **7**, 386 (2024).
- [22] C. Gidney, M. Newman, P. Brooks, and C. Jones, Yoked surface codes, *Nat. Commun.* **16**, 4498 (2025).
- [23] S.-H. Lee, L. English, and S. D. Bartlett, Efficient post-selection for general quantum ldpc codes, [arXiv:2510.05795](https://arxiv.org/abs/2510.05795) (2025).
- [24] H. Xie, N. Yoshioka, K. Tsubouchi, and Y. Li, Simple, efficient, and generic post-selection decoding for qldpc codes, [arXiv:2601.17757](https://arxiv.org/abs/2601.17757) (2026).
- [25] K. Kishi, R. Toshio, J. Fujisaki, H. Oshima, S. Sato, and K. Fujii, Even more efficient soft-output decoding with extra-cluster growth and early stopping, [arXiv preprint arXiv:2602.03336](https://arxiv.org/abs/2602.03336) (2026).
- [26] Z. Zhou, S. Pexton, A. Kubica, and Y. Ding, Error mitigation of fault-tolerant quantum circuits with soft information, [arXiv:2512.09863](https://arxiv.org/abs/2512.09863) (2025).
- [27] M. Dincă, T. Chan, and S. C. Benjamin, Error mitigation for logical circuits using decoder confidence, [arXiv:2512.15689](https://arxiv.org/abs/2512.15689) (2025).
- [28] D. Aharonov, Y. Atia, E. Bairey, Z. Brakerski, I. Cohen, O. Golan, I. Gurwich, N. H. Lindner, and M. Shutman, Syndrome aware mitigation of logical errors, [arXiv:2512.23810](https://arxiv.org/abs/2512.23810) (2025).
- [29] R. Takagi, S. Endo, S. Minagawa, and M. Gu, Fundamental limits of quantum error mitigation, *npj Quantum Inf.* **8**, 114 (2022).
- [30] R. Takagi, H. Tajima, and M. Gu, Universal sampling lower bounds for quantum error mitigation, *Phys. Rev. Lett.* **131**, 210602 (2023).
- [31] K. Tsubouchi, T. Sagawa, and N. Yoshioka, Universal cost bound of quantum error mitigation based on quantum estimation theory, *Phys. Rev. Lett.* **131**, 210601 (2023).
- [32] Y. Quek, D. Stilck França, S. Khatiri, J. J. Meyer, and J. Eisert, Exponentially tighter bounds on limitations of quantum error mitigation, *Nat. Phys.* **20**, 1648 (2024).
- [33] C. W. Helstrom, Quantum detection and estimation theory, *J. Stat. Phys.* **1**, 231 (1969).
- [34] A. S. Holevo, *Probabilistic and statistical aspects of quantum theory*, Vol. 1 (Springer Science & Business Media, 2011).
- [35] M. Hayashi, *Quantum information* (Springer, 2006).
- [36] J. Suzuki, Y. Yang, and M. Hayashi, Quantum state estimation with nuisance parameters, *Journal of Physics A: Mathematical and Theoretical* **53**, 453001 (2020).
- [37] Y. Yang, G. Chiribella, and M. Hayashi, Attaining the ultimate precision limit in quantum state estimation, *Commun. Math. Phys.* **368**, 223 (2019).
- [38] S. Zhou, C.-L. Zou, and L. Jiang, Saturating the quantum cramer-rao bound using locc, *Quantum Sci. Technol.* **5**, 025005 (2020).
- [39] G. Kimura, The bloch vector for n-level systems, *Phys. Lett. A* **314**, 339 (2003).
- [40] P. Iyer and D. Poulin, Hardness of decoding quantum stabilizer codes, *IEEE Trans. Inf. Theory* **61**, 5209 (2015).
- [41] P. Fuentes, J. E. Martinez, P. M. Crespo, and J. Garcia-Frías, Degeneracy and its impact on the decoding of sparse quantum codes, *IEEE Access* **9**, 89093 (2021).
- [42] A. deMarti iOlius, P. Fuentes, R. Orús, P. M. Crespo, and J. E. Martinez, Decoding algorithms for surface codes, *Quantum* **8**, 1498 (2024).
- [43] Y. Watanabe, T. Sagawa, and M. Ueda, Optimal measurement on noisy quantum systems, *Phys. Rev. Lett.* **104**, 020401 (2010).
- [44] Y. Li and S. C. Benjamin, Efficient variational quantum simulator incorporating active error minimization, *Phys. Rev. X* **7**, 021050 (2017).
- [45] S. Endo, S. C. Benjamin, and Y. Li, Practical quantum error mitigation for near-future applications, *Phys. Rev. X* **8**, 031027 (2018).
- [46] E. Van Den Berg, Z. K. Mineev, A. Kandala, and K. Temme, Probabilistic error cancellation with sparse pauli-lindblad models on noisy quantum processors, *Nat. Phys.* **19**, 1116 (2023).
- [47] X. Bonet-Monroig, R. Sagastizabal, M. Singh, and T. E. O'Brien, Low-cost error mitigation by symmetry verification, *Phys. Rev. A* **98**, 062339 (2018).
- [48] S. McArdle, X. Yuan, and S. Benjamin, Error-mitigated digital quantum simulation, *Phys. Rev. Lett.* **122**, 180501 (2019).
- [49] P. Czarnik, A. Arrasmith, P. J. Coles, and L. Cincio, Error mitigation with clifford quantum-circuit data, *Quantum* **5**, 592 (2021).
- [50] A. Strikis, D. Qin, Y. Chen, S. C. Benjamin, and Y. Li, Learning-based quantum error mitigation, *PRX Quantum* **2**, 040330 (2021).

- [51] A. Paetznick, M. Da Silva, C. Ryan-Anderson, J. Bello-Rivas, J. Campora III, A. Chernoguzov, J. Dreiling, C. Foltz, F. Frachon, J. Gaebler, *et al.*, Demonstration of logical qubits and repeated error correction with better-than-physical error rates, [arXiv:2404.02280 \(2024\)](#).
- [52] E. Dennis, A. Kitaev, A. Landahl, and J. Preskill, Topological quantum memory, *J. Math. Phys.* **43**, 4452 (2002).
- [53] O. Higgott and C. Gidney, Sparse blossom: correcting a million errors per core second with minimum-weight matching, *Quantum* **9**, 1600 (2025).
- [54] P. Pantelev and G. Kalachev, Degenerate quantum ldpc codes with good finite length performance, *Quantum* **5**, 585 (2021).
- [55] J. Roffe, D. R. White, S. Burton, and E. Campbell, Decoding across the quantum low-density parity-check code landscape, *Phys. Rev. Res.* **2**, 043423 (2020).
- [56] T. Müller, T. Alexander, M. E. Beverland, M. Bühler, B. R. Johnson, T. Maurer, and D. Vandeth, Improved belief propagation is sufficient for real-time decoding of quantum memory, [arXiv:2506.01779 \(2025\)](#).
- [57] K. Tsubouchi, H. Yamasaki, and S. Tamiya, Degeneracy cutting: A local and efficient post-processing for belief propagation decoding of quantum low-density parity-check codes, [arXiv:2510.08695 \(2025\)](#).
- [58] A. Hutter, J. R. Wootton, and D. Loss, Efficient markov chain monte carlo algorithm for the surface code, *Phys. Rev. A* **89**, 022326 (2014).
- [59] C. Gidney, Stim: a fast stabilizer circuit simulator, *Quantum* **5**, 497 (2021).
- [60] O. Higgott and C. Gidney, Sparse Blossom: correcting a million errors per core second with minimum-weight matching, *Quantum* **9**, 1600 (2025).
- [61] M. Jeon and Z. Cai, Quantum error correction on error-mitigated physical qubits, [arXiv:2601.18384 \(2026\)](#).
- [62] A. A. Mele, Introduction to haar measure tools in quantum information: A beginner's tutorial, *Quantum* **8**, 1340 (2024).